LEVEL II

AD A103943

RADC-TR-81-40
In-House Report
March 1981

BASIC DESIGN PRINCIPLES OF ELECTROMAGNETIC SCATTERING MEASUREMENT FACILITIES

Richard B. Mack

ROME AIR DEVELOPMENT CENTER
Air Force Systems Command
Griffiss Air Force Base, New York 13441

This report has been reviewed by the RADC Public Affairs Office (PA) and is releasable to the National Technical Information Service (NTIS). At NTIS it will be releasable to the general public, including foreign nations.

RADC-TR-81-40 has been reviewed and is approved for publication.

APPROVED: Philipp Blacksmith

PHILIPP BLACKSMITH, Branch Chief
EM Techniques Branch
Electromagnetic Sciences Division

APPROVED: Allan C. Schell

ALLAN C. SCHELL, Chief
Electromagnetic Sciences Division

FOR THE COMMANDER: John P. Huss

JOHN P. HUSS
Acting Chief, Plans Office

If your address has changed or if you wish to be removed from the RADC mailing list, or if the addressee is no longer employed by your organization, please notify RADC (EEC), Hanscom AFB MA 01731. This will assist us in maintaining a current mailing list.

Do not return this copy. Retain or destroy.

Unclassified

SECURITY CLASSIFICATION OF THIS PAGE (When Data Entered)

REPORT DOCUMENTATION PAGE		READ INSTRUCTIONS BEFORE COMPLETING FORM
1. REPORT NUMBER RADC-TR-81-40	2. GOVT ACCESSION NO. AD-A103 943	3. RECIPIENT'S CATALOG NUMBER
4. TITLE (and Subtitle) BASIC DESIGN PRINCIPLES OF ELECTROMAGNETIC SCATTERING MEASUREMENT FACILITIES		5. TYPE OF REPORT & PERIOD COVERED In-House Report 6. PERFORMING ORG. REPORT NUMBER N/A
7. AUTHOR(s) Richard B. Mack*		8. CONTRACT OR GRANT NUMBER(s) N/A
9. PERFORMING ORGANIZATION NAME AND ADDRESS Deputy for Electronic Technology (RADC/EEC) Hanscom Air Force Base Massachusetts 01731		10. PROGRAM ELEMENT, PROJECT, TASK AREA & WORK UNIT NUMBERS 61102F 23055440
11. CONTROLLING OFFICE NAME AND ADDRESS Deputy for Electronic Technology (RADC/EEC) Hanscom Air Force Base Massachusetts 01731		12. REPORT DATE March 1981 13. NUMBER OF PAGES 79
14. MONITORING AGENCY NAME & ADDRESS(if different from Controlling Office) 9 Technical Rpts		15. SECURITY CLASS (of this report) Unclassified 15a. DECLASSIFICATION/DOWNGRADING SCHEDULE N/A

16. DISTRIBUTION STATEMENT (of this Report)

Approved for public release; distribution unlimited.

17. DISTRIBUTION STATEMENT (of the abstract entered in Block 20, if different from Report)

18. SUPPLEMENTARY NOTES

*Formerly RADC

RADC Project Engineer: Ronald G. Newburgh (EEC)

19. KEY WORDS (Continue on reverse side if necessary and identify by block number)

Electromagnetic scattering
Radar cross sections

20. ABSTRACT (Continue on reverse side if necessary and identify by block number)

Typical experimental configurations that are used for measuring radar scattering are analyzed with simplified forms of basic electromagnetic principles to show how the experimental facility design affects measurement capability and the accuracy of the measured results. The discussion includes effects of a nonuniform field over the model space, the measurement distance from the scattering model, multiple reflections from walls of a chamber or from nearby objects, interference from model support structures, and the

DD FORM 1 JAN 73 1473 EDITION OF 1 NOV 65 IS OBSOLETE

Unclassified

SECURITY CLASSIFICATION OF THIS PAGE (When Data Entered)

309050

Unclassified

SECURITY CLASSIFICATION OF THIS PAGE(When Data Entered)

20. Abstract (Continued)

effects of forward scattering. Guiding principles are developed for choosing and designing the important components of a scattering measurement facility such as the transmit/receive antennas, the rf power sources, model support structures, and transmission line component assemblies so that measurement accuracy is maximized. Simple experimental procedures are given for evaluating a given measurement setup. Emphasis in the report is placed on illustrating the principles with numerical examples.

Unclassified

SECURITY CLASSIFICATION OF THIS PAGE(When Data Entered)

Contents

Contents

Illustrations

Illustrations

Tables

BLANK PAGE

Basic Design Principles of Electromagnetic Scattering Measurement Facilities

1. INTRODUCTION

The purpose of this technical report is to examine the basic electromagnetic principles that govern the design of electromagnetic scattering measurement facilities. Special emphasis is placed on the practical application of the principles and on their practical meaning in determining the effects of the facility design on measurement accuracy. Although the discussions are not specifically restricted to any frequency range, they are implicitly directed toward the frequency range of 1 GHz to 40 GHz.

Likewise, most of the discussions apply to short pulse or other types of scattering measurements but are implicitly directed toward CW cancellation systems. The principles discussed apply equally to measurements made on an outdoor facility or to measurements on an indoor range where the free space environment is approximated by a microwave anechoic chamber. Ideally, the overall design parameters of the facility would be dictated by the types of measurements anticipated, the model sizes, frequency ranges, cross section levels, the degree of automation desired, etc. In reality, such parameters can rarely be specified in advance. When the facility is to be used in an R & D environment the anticipation of future desirable projects is even less precise. In such a situation it is well to recall that an arbitrarily imposed set of design parameters is in fact an advanced statement

(Received for publication 19 February 1981)

of what the facility will never be capable of measuring. The importance of this consideration is that a specified set of design parameters can frequently be met by restrictive designs that largely prohibit the facility's even occasional use for projects that fall outside of the original parameters.

The alternative approach is to design the facility for maximum versatility, and this design philosophy is generally followed in the present discussion.

There are some implications of the "design for maximum versatility" philosophy. For example, the advantages in terms of minimum measurable cross sections of being able to measure a model at the shortest range consistent with being in the model's far field are discussed in the next section. If the chamber design is focused on producing a quiet zone of some limited volume centered at one spot of the chamber, the advantages of optimizing the measurement range for each scatterer are lost. Similarly, if cheaper absorber of lower quality or having polarization sensitivity is used on side walls of the chamber, the ability to make measurements at bistatic angles or with other than horizontal and vertical polarizations may be severaly limited. The net result is that a versatile chamber to be used for electromagnetic (EM) scattering measurements cannot take full advantage of recent advances in chamber design.

Note that in this respect, the requirements for a scattering measurement range and, in particular, for an anechoic chamber to be used for scattering measurements, differ from those of an antenna measurement range or chamber. The antenna case involves one way propagation paths, generally much higher power levels at the receiver, and never requires bistatic measurements. Hence, the quiet zone approach to design of an antenna range or chamber can lead to a very versatile facility.

The frequency range is another fundamental consideration. The discussion herein is directed toward operation over the band of 1 GHz to 40 GHz. The general guides for these limits are that smaller targets can be measured without modeling at L-Band, while larger real system targets, such as airplanes viewed with an L-Band radar, require high model measurement frequencies if the scaled model is to be of a convenient size. For example, since scaling is linear with wavelength, a 40 ft target at 1 GHz becomes a 1 ft model at 40 GHz.

The required far field measurement distance is proportional to the square of the maximum dimension of the model and inversely proportional to the wavelength and, hence, only 1/40 of that required for the full scatterer in the above example.

An additional consideration in choosing the general frequency range is that, based on the manufacturer's literature, pyramidal absorber with reflectivity levels specified at 1 GHz first improves as the frequency is increased, but then deteriorates in performance as the frequency is raised, until, at 40 GHz its reflectivity is approximately the same as at 1 GHz. In addition, a -40 dB reflectivity level

specified at 1 GHz still permits useful but lower quality measurements in the chamber down to 300 MHz.

An electromagnetic scattering measurement facility can be divided into the following set of subsystems:

1. The range (or chamber)
2. Model mounts
3. Transmit/Receive antennas
4. RF transmitting sources
5. RF plumbing
6. Receiving equipment
7. Data handling equipment

Each subsystem has its own set of technical requirements and design tradeoffs within the constraints of the overall facility parameters. An understanding of the individual subsystem tradeoffs will frequently permit a combination of them to be played against each other to yield more accurate results, or even to permit reliable measurements of scatters that could not be accommodated by a given facility if a rigid application of fixed criteria were made.

Section 2 gives a brief review of the basic laws governing the accuracy of radar scattering measurements, and of the laws that define the measurement capability of a given facility. The following sections contain detailed discussions of each subsystem except the receiving equipment and the data handling equipment. Choice of receiving and data handling equipment are basically not electromagnetic concerns and are determined primarily by state of the art commercial products that are available within budgetary constraints. Primary requirements of the receiver are that it be stable and very sensitive. Typical commercial receivers currently available have minimum detectable signal levels of -70 dBm at 40 GHz improving to -110 to -120 dBm at 1.0 GHz and these are very suitable. The receiver also should be capable of measuring phase as well as power or amplitude, and should have outputs that are compatible with existing analog recorders for recording both phase and amplitude. It is also highly desirable that the receiving equipment have a capability of at least digitally storing the input data on tape for later computer processing, because nearly all measured scattering data is relative data and frequently requires normalization and scaling to actual operational frequencies.

2. BASIC EM SCATTERING PRINCIPLES

The production of high quality measured data from a given scattering measurement facility requires the careful application of only a few relatively simple rules, but these basic rules must be applied with understanding if good results are to be

obtained with even the highest quality facility. These basic principles, in turn, impinge on the facility design because the facility should be designed, insofar as possible, within limitations of physical and budgeting restraints to enhance the measured results.

The basic principles that govern scattering measurements are summarized below and discussed in the following subsections. Examples given are specifically for free space backscatter facilities but appropriate versions of the principles apply to all types of EM scattering facilities.

The principles are:

1. Linear passive electromagnetic systems can be scaled up or down in frequency, with linear dimensions scaled directly proportional to the wavelength or inversely as the frequency. Areas scale as the square of the wavelength or inversely as the square of the frequency.

2. Measurements of the scattered fields must be made in the far field of the scattering target.

3. The incident field over the space to be occupied by the scatterer must be a close approximation to a plane wave.

4. Background signals from wall reflections, leakage, etc., must be reduced by some means to levels that do not introduce unacceptable errors into the lowest cross sections to be measured. The reduced levels of background signal must be maintained during the course of a measurement.

5. Power relationships in EM scattering measurements are governed by the radar equation. For a given experimental setup this equation defines the smallest cross section that can be measured with a specified error.

2.1 Electromagnetic Similitude

The laws of electromagnetic similitude say that electromagnetic systems will give equivalent results at any frequency as long as all linear dimensions of the system are scaled in an inverse proportion to the frequency. In air, linear dimensions are simply directly proportional to the wavelength.

This simple property of electromagnetic systems makes possible the use of model measurement ranges. For example, a real radar target having a maximum dimension of 40 ft will yield the same relative scattering pattern at L-Band (1 GHz) as an accurately constructed model having 1 ft maximum dimensions and measured at 40 GHz. Similarly, a 4 ft model could be used at 10 GHz or a 20 ft model at 2 GHz. The relationship[1] is

---

1. Blacksmith, P., Hiatt, R.E., and Mack, R.B. (1965) Introduction to radar cross section measurements, Proc. IEEE 53:901-920.

$$L_2 = (\lambda_2/\lambda_1)L_1 = (f_1/f_2)L_1 \qquad (1)$$

where L_2 represents linear model dimensions at frequency f_2 and wavelength λ_2, and L_1 represents linear model dimensions at frequency f_1 and λ_1. Clearly, linear media and linear materials are assumed.

The word "accurately" is underlined because it is an important key to measuring the same scattering pattern with different models scaled to represent different real operating frequencies. Accurately means all of the details including the interior of openings, gaps, stores, and any surface over which surface fields can exist and contribute to the reradiated field. Accurately also means tolerances and these also scale according to Eq. (1). Thus, if the model is to represent a real scatterer within $\lambda/20$, tolerances of an X-Band (10 GHz) model must be ±0.050 in. and tolerances of a 40 GHz model must be no poorer than ±0.0125 in.

The costs of constructing a model are at least inversely proportional to the tolerances. Hence, it is common practice to make estimates of details that are too small to affect the scattering pattern, and to estimate the effects of reduced tolerances on major features of the scattering pattern prior to specifying the model's tolerances.

Real radar targets at UHF, VHF, and HF have many details that do not contribute significantly to the scattering pattern, and can therefore be represented by very simple models. However, at L-Band and higher frequencies, nearly all details contribute and must be included in the model if the model is to be an accurate representation of the real target.

A statement commonly made is that there is generally poor agreement between the relative scattering patterns from a model measurement and those from the real scatterer. The differences are very frequently caused by failure to include sufficient details and accuracy in the model.

As applied to radar scattering measurements, Eq. (1) is used three ways. First, if a fixed model measurement frequency is available, Eq. (1) defines the model size to represent a full size system at a given full size radar frequency. Secondly, if a model is available, Eq. (1) defines the measurement frequency to represent a given full size target and radar. Thirdly, if model measurement results are already available from a model of given size measured at a given model frequency, Eq. (1) defines the full system target size and radar frequency to which the results apply.

The absolute radar cross section of a scatterer is an area and hence, varies as the square of the wavelength or inversely, as the square of the frequency for scaled systems,

$$\sigma_2 = (\lambda_2/\lambda_1)^2 \sigma_1 = (f_1/f_2)^2 \sigma_1 \qquad (2)$$

where σ_2 is the radar cross section at frequency f_2 and wavelength λ_2 and σ_1 is the radar cross section at frequency f_1 and wavelength λ_1. Note that while scaling EM scattering systems for measurements to higher frequencies offers the advantage of smaller models, the higher frequency model range must be capable of measuring smaller cross sections. For example, a low cross section target at L-Band (1 GHz) might have an radar cross section (RCS) of 0.1 m^2 at some aspect. At X-Band (10 GHz) its model's RCS at this aspect would be 10^{-3} m^2, and at 40 GHz an appropriately scaled model would have an RCS of 0.25 (10^{-5}) m^2. An airplane might have an RCS of 400 m^2 at some aspect. Its X-Band model would have an RCS of 4 m^2 at the same aspect and its 40 GHz model an RCS of 0.25 m^2.

2.2 The Far Field of the Model

The relative scattering patterns and the radar cross sections of the model must be measured at a sufficient distance R from the model to insure that the measured results are independent of R. This is commonly referred to as being in the far field of the model.

Mathematical statements of the far field requirements are easily derived from the Kirchoff-Huygens formulation for calculating the scattered fields.[2,3] In this formulation the scattered magnetic field is given by

$$\vec{H}^s = -\frac{1}{4\pi} \int_S [(\hat{n} \times \vec{H}_t) \times \nabla e^{-ikr}/r] \, dS \qquad (3)$$

where the surface of integration is the surface of the scatterer and a closed surface at infinity (over which the integral is zero), $\hat{n}$ is a unit normal to the surface, $\vec{H}_t$ is the total tangential field on the surface of the scatterer, and r is the distance from the observation of measurement point, the transmit/receive antenna of a model backscattering range, to a current element on the surface of the scatterer. Equation (3) contains no approximations, it gives the scattered field everywhere outside of a perfectly conducting scatterer.

---

2. Silver, S. (1949) Microwave Antenna Theory and Design, Vol. 12, Radiation Laboratory Series, McGraw-Hill Book Company, Chap. 6.
3. Kerr, D.E. (1951) Propagation of Short Radio Waves, Vol. 13, Radiation Laboratory Series, McGraw-Hill Book Company, Chapts. 4 and 6.

Consider the gradient:

$$\nabla\left(\frac{e^{-ikr}}{r}\right) = -e^{-ikr}\,\hat{n}_o\left[\frac{ik}{r} + \frac{1}{r^2}\right] \tag{4}$$

and the scattered field becomes

$$\vec{H}^s = -\frac{1}{4\pi}\int_s\left[\hat{n}_o \times (\hat{n} \times \vec{H}_t)\left(\frac{ik}{r} + \frac{1}{r^2}\right) e^{-ikr}\right] dS \quad . \tag{5}$$

Since we are interested in the field at relatively large distances from the scatterer, little error is introduced by replacing r by R, the distance from the measurement point to the center of the scatterer, in the amplitude. R is independent of the integration so that

$$\vec{H}^s = -\frac{1}{4\pi}\left[\frac{ik}{R} + \frac{1}{R^2}\right]\int_s [\hat{n}_o \times (\hat{n} \times \vec{H}_t)\, e^{-ikr}]\, dS \quad . \tag{6}$$

Thus, in general there exist two components of the scattered field which differ in phase by 90^o.

The phase requires a more delicate treatment. From Figure 1 the difference in path length to a measurement point located a distance R from the center of the scatterer between a current element at the center of the scatterer and one at x' is ℓ so that

$$r = R + \ell = (R^2 + x'^2)^{1/2} = R(1 + x'^2/R^2)^{1/2} = R(1 + x'^2/2R^2) \tag{7a}$$

$$= R + x'^2/2R \quad . \tag{7b}$$

Then the field becomes

$$\vec{H}^s = -\frac{1}{4\pi}\,(ik + 1/R)\,\frac{e^{-ikR}}{R}\int_s [\hat{n}_o \times (\hat{n} \times \vec{H}_t)]\, e^{-ikx'^2/2R}\, dS \quad . \tag{7c}$$

Since the scattered field at any measurement point is complex with both an amplitude and a phase, separate conditions must be placed on each to insure that the measurement distance from the scatterer is sufficient to guarantee that there is

only one dominant component and that the range-dependent quadratic phase variation is negligible.

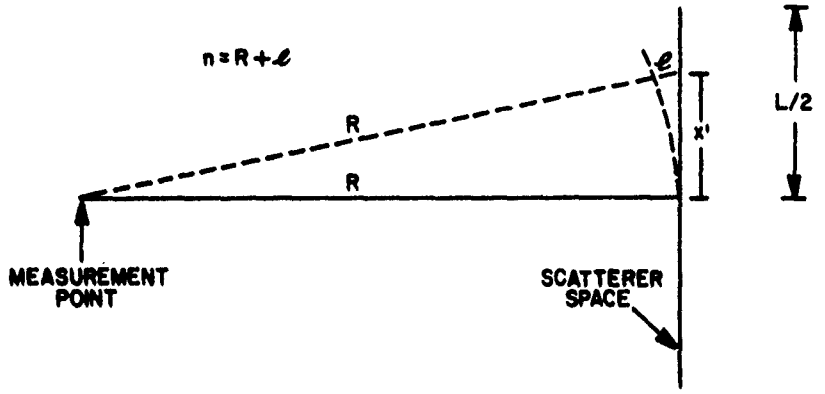

Figure 1. Geometry for Determining Phase Error Due to Finite Measurement Distance

The ratio of the amplitude of the $1/R^2$ to the $1/R$ components is

$$R_R = \lambda/(2\pi R) \quad , \tag{8a}$$

$$R_{R\ dB} = -16 - 20 \log R/\lambda \quad . \tag{8b}$$

For the phase term, the assumption that the largest phase errors come from the extremities of the scatterer where $x' = L/2$ leads to

$$\ell = L^2/8R \quad . \tag{9a}$$

If it is further assumed that a quadratic phase error of 22.5° corresponding to path differences of $\ell = \lambda/16$ is acceptable,

$$R = 2L^2/\lambda \quad \text{(conventional far field)} \quad . \tag{9b}$$

For this far field condition, the ratio of the amplitude components is

$$R_R = -22 - 40 \log L/\lambda \qquad (R = 2L^2/\lambda) \quad . \tag{9c}$$

Except in cases where the conventional far field criterion is applied to scatterers that are small compared to the wavelength, its application generally insures that the $1/R^2$ components are negligible compared to the $1/R$ components of the field. For example, if $\ell/\lambda = 1$, $R_R = -22$ dB and the error created in the measured cross section is (see Blacksmith, et al,[1] Figure 3) approximately ±0.75 dB; for $L/\lambda = 2$, $R_R = -34$ dB and the possible error in measured cross sections is approximately ±0.2 dB. If the scatterer has three or more wavelengths in its maximum dimension, measurements at distances specified by the conventional criteria will result in errors of ±0.1 dB or less in measured cross sections due to the neglected field components.

Whether the criterion of Eq. (9b) is sufficient to keep the quadratic error within acceptable limits depends on how heavily the scatter in question weights the current elements at its extremities. For a given scatterer this also is a function of the orientation of the scatterer, in general.

Figure 2 shows examples of quadratic phase error due to finite measurement distances in the backscatter pattern of a square flat metal plate of 10λ on a side. Patterns in Figure 2 were calculated from physical optics[2, 3] for distances $R = p$ with $p = 1/2$, 1, 2, 4, and infinity. As can be seen from Figure 2 the largest errors are introduced near the first null and first side lobe of the scattering patterns. Even at substantially reduced distances, the error effects decrease at angles away from the broadside direction, even though the overall pattern levels are lower at the SE angles. Also, doubling of the measurement distance increases the null depths by approximately 6 dB.

Beyond the center of the first side lobe through the third side lobe the pattern at $R = 2L^2/\lambda$ gives a pattern that is within 0.5 dB of the ideal one except very near the nulls; at angles beyond the third side lobe the approximation is better. Similarly, the criterion $R = L^2/\lambda$ gives a pattern within approximately 1 dB of the ideal one at and beyond the first side lobe the approximation is better. Similarly, the criterion $R = L^2/2\lambda$ gives a pattern within approximately 1 dB of the ideal one at and beyond the first side lobe except near the nulls. Effects of the quadratic error on the pattern broadside maximum are summarized in Table 1.

Note that the preceding discussion of backscatter from a square plate assumes the incident field to be a planewave and only the receiving distance to be finite.

Experimentally, it is usually very simple to determine if a given measurement distance R is sufficient to obtain a scattering pattern within a desired error tolerance. The procedure is to measure the pattern at a chosen distance, move the scatterer toward or away from the transmit/receive antenna and remeasure the pattern. If pattern differences are within acceptable limits, the closer distance is adequate. This procedure is especially useful when scattering patterns must be

measured over a wide power range and the lower powers are too close to the receiver noise level to permit use of the conventional far field criterion.

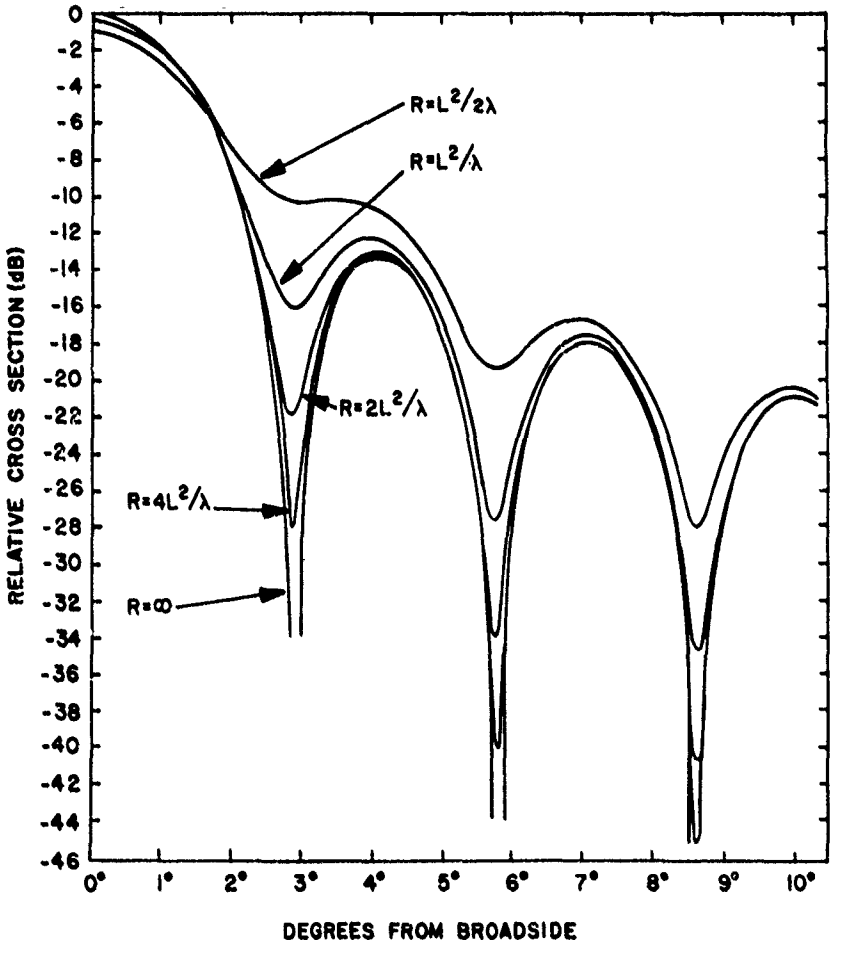

Figure 2. Backscatter Pattern of 10λ Square Plate at Various Measurement Distances

Table 1. Error in Maximum of Backscatter Pattern Due to Finite Measurement Distance

(Scatterer: 10λ sq. plate)			
Measurement Distance (R)	Phase Error (Deg)	Path Length Error (λ)	Pattern Max Compared To Ideal (dB)
$L^2/2\lambda$	90°	$\lambda/4$	-0.89
L^2/λ	45°	$\lambda/8$	-0.24
$2L^2/\lambda$	22.5°	$\lambda/16$	-0.05
$4L^2/\lambda$	11.25	$\lambda/32$	-0.014

2.3 The Incident Field Over the Model Space

The incident field over the volume of space to be occupied by the model should be a good approximation to a planewave. This requirement reduces to

$$\frac{E_L(R - L/2) - E_L(R + L/2)}{E_L(R)} \leq \delta E_L \quad , \tag{10a}$$

$$E_T(0) - E_T(\theta) \leq \delta E_T \quad , \tag{10b}$$

$$\phi_T(0) - \phi_T(\theta) \leq \delta\phi_T \quad , \tag{10c}$$

where δE_L is the acceptable fractional radial variation in the amplitude of the incident field over the model space; δE_T and $\delta\phi_T$ are, respectively, the acceptable transverse variations in amplitude and phase over the model space; and R is the distance from the transmit/receive antenna to the center of the model. The angle is given by

$$\theta = \tan^{-1} L/2R \quad . \tag{11}$$

Consider first the radial variation of field over a model of largest dimension L. Assuming a 1/R field dependence, Eq. (10a) gives

$$\delta E_L = \frac{1/(R - L/2) - 1/(R + L/2)}{1/R} = \frac{L/R}{1 - (L/2R)^2} \qquad (12a)$$

$$\doteq L/R \quad . \qquad (12b)$$

The transverse field is given by the antenna pattern of the transmit/receive antenna. For a circular aperture and uniform illumination the pattern is given by Skolnik (Chapter 7)[4]

$$E_{TC} = \frac{J_1\left(\frac{\pi D}{\lambda} \sin\theta\right)}{\left(\frac{\pi D}{\lambda} \sin\theta\right)} \quad . \qquad (13)$$

Using small angle formulas,

$$\sin\theta \doteq \theta = \tan^{-1} L/2R \doteq \theta$$

so that

$$E_{TC} = \frac{J_1\left(\frac{\pi D}{\lambda} \cdot \frac{L}{2R}\right)}{\left(\frac{\pi D}{\lambda} \cdot \frac{L}{2R}\right)} \qquad \text{(circular aperture uniform illumination)} \qquad (14a)$$

$$\delta E_{TC} = 1 - E_{TC} \quad . \qquad (14b)$$

Half power beamwidths are given by

$$\theta_{1/2C} \doteq (58.5\,\lambda/D)^{\circ} \qquad \text{(circular aperture uniform illumination)} \qquad (14c)$$

A useful series for $J_1(x)/x$ is

$$\frac{J_1(x)}{x} = 1 - \frac{x^2}{8} + \frac{x^4}{8 \cdot 24} - \frac{x^6}{2 \cdot 24 \cdot 48} + \cdots \quad . \qquad (15)$$

---

4. Skolnik, M. I. (1962) Introduction to Radar Systems, McGraw-Hill Book Company, Chapts. 1 and 7.

The phase is typically nearly constant across the main beam out to the half power points. Hence, if the amplitude illumination is smooth over the scatterer space the phase will also be smooth.

Many combinations can be used to satisfy Eqs. (10a) to (10c) and all are legitimate as long as the far field distances of the scattering model are not violated. These include measurements in the near field of the antenna if the model is small, or the antenna focused in the near field with the scattering model located at the focal region.

The actual criteria for Eqs. (10a) to (10c) are difficult to specify for a given model because final effects on the measured results depend on the model's weighting of the field. Even for a given model weights will depend upon the orientation of the model with respect to the transmit/receive antenna.

A great deal has been written on this subject; the objective of most has been to establish universal criteria for automatically insuring adequate fields over the model space. The problem with such universal criteria is that they are either too restrictive in any individual case and actually degrade results by requiring excessive R's, or they introduce errors in the measurements by ignoring the radial changes of the field.

The most widely accepted criterion is that the measurements should be in the far field of the transmit/receive antenna. Under this restriction, the minimum distance from the transmit/receive antenna for measurements is

$$R = R_{min} = 2D^2/\lambda \tag{16}$$

where D is the maximum dimension of the antenna. With Eq. (16) E_{TC} becomes

$$E_{TC} = \frac{J_1\left(\frac{\pi}{4} \cdot \frac{L}{D}\right)}{\left(\frac{\pi}{4} \cdot \frac{L}{D}\right)} , \qquad \begin{matrix}\text{(circular aperture uniform illumination)} \\ (R = 2D^2/\lambda)\end{matrix} \tag{17}$$

The radial condition becomes

$$\delta E_L \pm \frac{L\lambda}{2D^2} .$$

An appreciation of the magnitude of Eqs. (17) and (18) is best obtained by several examples:

1. A 12 in. model is to be measured at 10 GHz (λ = 1.18 in.) with a 12 in. antenna.

$$R = 2D^2/\lambda = 20.3 \text{ ft}$$

$$\delta E_L = \frac{12\,(1.18)}{2(12)^2} = 0.049 = -44 \text{ dB}$$

$$\delta E_{TC} = 1 - \frac{J_1(\pi/4)}{(\pi/4)} = 0.08 = 0.68 \text{ dB} \quad .$$

2. A 12 in. model is to be measured at 10 GHz with a 24 in. antenna.

$$R = 2D^2/\lambda = 1.4 \text{ ft}$$

$$\delta E_L = \frac{12\,(1.18)}{2(24)^2} = 0.012 = -0.11 \text{ dB}$$

$$\delta E_{ro} = 1 - \frac{J_1(\pi/8)}{(\pi/8)} = 0.019 = -0.17 \text{ dB} \quad .$$

3. A 12 in. model is to be measured at 10 GHz with a 24 in. antenna but at the reduced range of $R = D^2/2\lambda$

$$R = D^2/2\lambda = 244.1 \text{ in.} = 20.3 \text{ ft.}$$

From Eqs. (14a) to (14c),

$$\delta E_T = 1 - \frac{J_1\left(\frac{\pi D}{\lambda} \cdot \frac{2L\lambda}{2D^2}\right)}{\left(\frac{\pi D}{\lambda} \cdot \frac{2\pi\lambda}{2D^2}\right)} = 1 - \frac{J_1(\pi L/D)}{(\pi L/D)} = 1 - \frac{J_1(\pi/2)}{(\pi/2)} = 0.278 = -2.83 \text{ dB}$$

$$\delta E_L = L/R = \frac{2\lambda L}{D^2} = 0.0492 = -0.44 \text{ dB} \quad .$$

In this case the model barely fits within the 3 dB points of the antenna beam, although the radial condition is well satisfied. In general the condition $R = 2D^2/\lambda$ is sufficient to insure small field changes over the model space but may not be necessary.

As a final point concerning the antenna fields consider the beamwidths, Eq. (14b) of Skolnik (Chapter 7)[4]

$$\theta_{1/2C} = 58.5\,\lambda/D = 1.02\,\lambda/D \text{ radians}$$

At a distance R from the antenna the 3 dB point of the beam covers a lateral extent ℓ of

$$\ell = 2R \tan \theta/2 = 2R\theta/2 = R\,\lambda/d \tag{19a}$$

With $R = 2D^2/\lambda$

$$\ell = (2D^2/\lambda)(\lambda/D) = 2D \tag{19b}$$

That is, at a distance of $R = 2D^2/\lambda$ from the antenna, the lateral distance between the 3 dB half power points of the beam is twice the antenna diameter. Similarly, at $R = D^2/\lambda$ the half power points cover a lateral distance equal to the antenna diameter. Note that this relation holds for uniform illumination; for tapered illumination the beams are wider.

Figure 3 illustrates the effects of placing a scatterer in a nonuniform incident field. The scatterer is a square metal plate of 10λ on a side and the results are calculated from physical optics.[2,3] The amplitude taper of the incident field of Figure 3 was assumed to be parabolic of the form

$$f(x) = 1 - (1 - \Delta) \cdot x^2$$

where x is the coordinate along one centerline of the plate, and the backscatter patterns are shown for values of Δ from 1 to 0.5. Principal effects of an incident field taper for this model are that the side lobes are reduced from the uniform case by approximately 1 dB for each 1 dB in total field taper, and the principal lobe is reduced by approximately 0.3 dB for each dB of field taper which also results in a slight broadening of the principal lobe.

2.4 Cancellation of the Background Signal

With all fields adjusted for minimum errors, the signal that arrives at the receiver with a scattering model in place consists of two parts. One part is the true signal reflected from the model while the second part is the sum of all background reflections, leakage signals, etc. Clearly, the second part is an error signal and should be much smaller than the true signal from the scatterer if reliable results are to be obtained.

After background signals have been reduced to a minimum by arrangement of the equipment, walls, mount, etc., the common practice is to introduce a signal

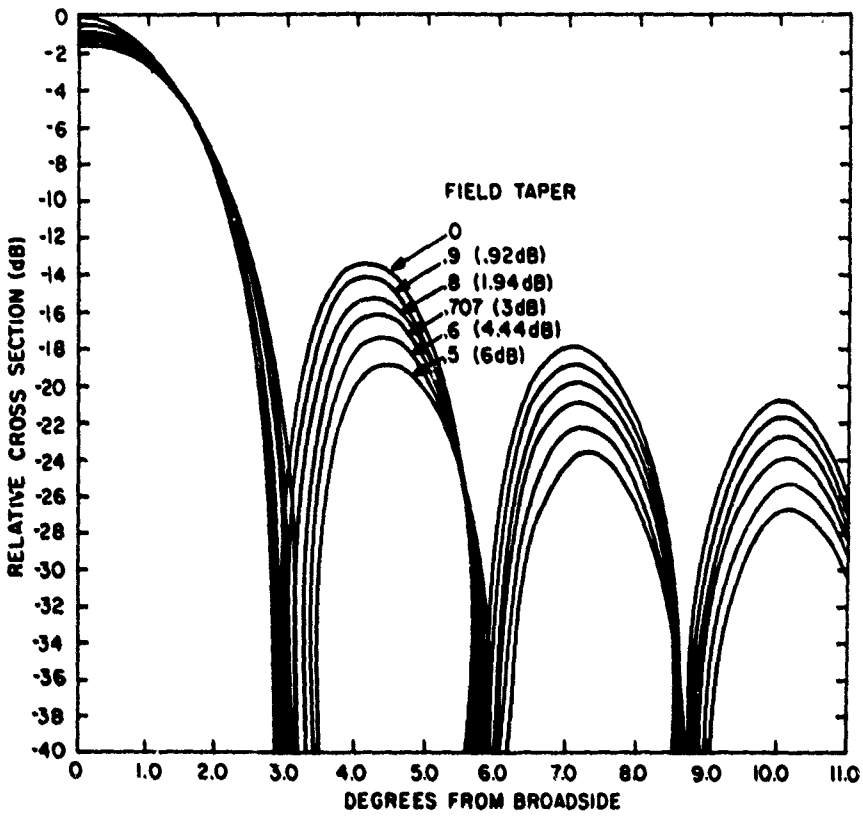

Figure 3. Backscatter Pattern of 10λ Square Plate in Various Field Tapers

directly from the transmitter into the receiving branch of the equipment and to adjust the phase and amplitude of this signal to cancel any remaining background signal. This step is carried out with the model removed from its mount and the cancellation must hold during the entire course of a measurement. Therefore, in the design of an experiment or facility, premium must be placed on rigidity of the walls, antennas, etc., and on the speed with which an individual measurement can be carried out. The transmitting source must also be stable. It is difficult to overemphasize the importance of short term mechanical stability of all parts of the anechoic chamber, the model mount, the transmit/receive antennas, all waveguide components, and the supporting structure for the transmission line components. The experiment must be designed to enable rapid placement and removal of the scatterer on its mount, and this should be carried out without moving the

structures such as ladders, etc. In other words, nothing in the chamber should move at all during the course of a measurement and standard reference measurement.

Letting subscript m represent the measured signal, t the true signal, and e the background error signal, [1]

$$e_m = e_t + e_e = e_t [1 + s_e e^{j\phi}] \tag{20}$$

where

$$s_e e^{j\phi} = e_e/e_t \quad . \tag{21}$$

The cross section is proportional to the square of the measured signal. Therefore,

$$\sigma = k e_m e_m^* = e_t e_t^* [1 + 2 s_e \cos \phi + s_e^2] \quad . \tag{22}$$

In dB

$$\sigma_{dB} = \sigma_{t\,dB} + \sigma_{e\,dB} \quad , \tag{23}$$

where

$$\sigma_{e\,dB} = 10 \log (1 + 2 s_e \cos \phi + s_e^2) \quad . \tag{24}$$

In Eq. (24), s_e^2 is usually negligible compared to the other two terms and the middle term fluctuates between $\pm 2 s_e$, introducing an error in the measured results, Eq. (23).

A graph of Eq. (24) showing the error introduced into measured results as a function of the ratio of background signal to the true signal, Eq. (21), is given in Reference 1.

Table 2. Scattering Pattern Errors for Various Cancellation Levels

(All values in dB)				
	Cancellation Level			
Pattern Level	-50	-60	-70	-40
0	0.1	0.1	0.1	±0.1
-10	±0.1	0.1	0.1	±0.3
-20	±0.3	±0.1	0.1	±1.0
-30	±1.0	±0.3	±0.1	±3.2
-40	±3.3	±1.0	±0.3	±7.2

For the following RCS errors, the cancellation level should be the indicated amount below the RCS level as given below:

Table 3. RCS Error vs Background Cancellation

(All values in dB)	
Error	Cancellation Level at Completion of Measurement
±0.25	-30
±0.5	-24
±1.0	-20
±2.0	-14

2.5 Model Range Power Relations

The power relationships on a model scattering range are governed by the radar equation,[4] which can be conveniently written as

$$P_r = \frac{P_t \alpha_t \alpha_r G^2 \lambda^2}{(4\pi)^3 R^4} \tag{25}$$

where

P_r = power received

P_t = power transmitted

α_t = attenuation of transmission line path

α_r = attenuation of receiving line path

G = antenna gain (assuming a single antenna for transmitting and receiving)

λ = wavelength

R = antenna-to-model distance

σ = radar cross section.

If a single transmit/receive antenna is used with a typical backscatter range, there will be a 3 dB loss on transmission and a 3 dB loss on reception through the

hybrid tee, and at least another dB of miscellaneous losses throughout the transmission line for a total of at least 8 dB.

The question that usually arises with regard to a model range is whether a given cross section level can be measured with an acceptable error using an available equipment. To answer this question, Eq. (25) is better solved for σ,

$$\sigma = \frac{P_r}{P_t} \frac{(4\pi)^3 R^4}{\alpha_r \alpha_t G^2 \lambda^2} \quad . \tag{26}$$

If P_r is taken to be the minimum measurable power, Eq. (26) defines the smallest cross section that can be measured with a given set of equipment parameters. Equation (26) is conveniently expressed in dB.

$$\boxed{\sigma_{dB} = 32.98 + (P_{r\,dBm} - P_{t\,dBm}) - \alpha_{T\,dB} - 2G_{dB} + 40 \log R - 20 \log \lambda} \tag{27}$$

where $P_{r\,dBm}$ and $P_{t\,dBm}$ are expressed in dB relative to one mW, $\alpha_{t\,dB}$ is the sum of the total transmission line losses ($\alpha_{t\,dB} + \alpha_{r\,dB} = \alpha_{T\,dB}$), G_{dB} is the antenna gain with respect to an isotropic radiator, and σ is in dB relative to 1 m^2. In the remainder of this report, $P_{r\,dBm}$ will be taken as the receiver sensitivity as stated by manufacturer's literature.

Equation (27) will be called the system sensitivity equation. It can readily be used to determine the minimum cross section that can be measured with a given arrangement.

A commonly used error tolerance in the measured cross section is ±1 dB; hence, when determining ϕ_{min}, 20 dB (see Table 3) will be added to the right side of Eq. (27) so that σ_{min} will be understood to mean the minimum measurable cross section with an error of ±1 dB. In this form

$$\boxed{\sigma_{min} = 53 + (P_{r\,dBm} - P_{t\,dBm}) - \alpha_{T\,dB} - 2G_{dB} - 40 \log R - 20 \log \lambda} \tag{28}$$

(system sensitivity equation) (±1 dB error)

As an example of the magnitudes involved, consider the following example, what is σ_{min} for a system with the following parameters:

f = 10 GHz (λ = 1.18 in. = 0.02997 m)

R = 10 m

$G = 30$ dB

$\alpha_t = -8$ dB

$P_t = 10$ dBm

$P_r = -100$ dBm

Solution

$$\sigma_{min} = 53 - 100 - 10 + 8 - 60 + 40 \log 10 - 20 \log (2.997 \times 10^{-2})$$

$$= -38.6 \text{ dBSM} = 1.395\ (10^{-4})\ m^2 \quad .$$

The importance of minimizing R is clear from Eq. (28). Reducing R by a factor of 2 improves the minimum measurable cross section by 12 dB; doubling R raises the minimum measurable cross section by 12 dB. Decreasing R by approximately 19 percent doubles the minimum measurable cross section.

There are fundamental differences between transmitter power levels and receiver sensitivities that are required for scattering measurements and those that are required for antenna testing. These differences make the scattering measurements much more difficult and are worth noting with a typical example of each.

Let the transmit antenna and the center of a quiet zone be separated by a distance R. The power density at the test space is (see Skolnik, Chapt. 1[4])

$$P = \frac{P_t G_t}{4\pi R^2} \quad . \tag{29}$$

A receiving antenna under test has an effective capture area A that absorbs part of this power. The antenna's capture area is related to its gain by

$$A_r = \frac{G_r \lambda^2}{4\pi} \tag{30}$$

The power at the receiver of an antenna under test is

$$P_{ra} = \frac{P_t G_t G_R \lambda^2}{(4\pi)^2 R^2} \qquad \text{(antenna test case)} \quad . \tag{31}$$

A scattering target reflects part of the incident energy, Eq. (29), back to the transmit antenna. The power received in the scattering case is

$$P_{rs} = \frac{P_t G^2 \lambda^2 \sigma}{(4\pi)^3 R^4} \qquad \text{(scattering measurement case)} . \tag{32}$$

Typical values for the antenna case might be

$P_t = 10$ mW

$G_t = 300$, $G_R = 300$

$\lambda = 0.02998$ m (10 GHz)

$R = 10$ m

$$P_{ra} = \frac{(10^{-2})(9)(10^4)(2.998)^2(10^{-4})}{(4\pi)^2 10^2}$$

(antenna case) .

$$= 0.51\ (10^{-4})\ \text{W}$$

For the scattering case typically σ might be 10^{-2} m^2. Therefore, using the other parameters as for the antenna case,

$$P_{rs} = \frac{(10^{-2})(9)(10^4)(2.998)^2(10^{-4})(10^{-2})}{(4\pi)^3 10^4}$$

(scattering measurement case) .

$$= 0.41\ (10^{-9})\ \text{W}$$

If the scatterers were an 8 in. model and located at its minimum far field distance of

$$R = 2D^2/\lambda = \frac{2(64)}{1.18} = 9 \text{ ft} = 3 \text{ m}$$

$$P_{rs} = \frac{81\ (10^{-4})}{(4\pi)^3\ (81)} = 0.50\ (10^{-7})\ \text{W} .$$

3. THE CHAMBER

The fundamental purpose of a microwave anechoic chamber is to simulate free space conditions by reducing or eliminating reflections that otherwise would be encountered from walls, ceilings, floors, and similar obstacles in an indoor measurement space and from buildings, trees, utility lines, etc., in an outdoors measurement space. Even though interior walls are lined with high quality microwave absorber there are still residual reflections that ultimately tend to limit the accuracy of EM measurements that are carried out in a chamber. These residual reflections come about because all microwave absorber has limited absorbability and because the effectiveness of the absorber generally decreases at grazing reflection angles.

Current practices in chamber design arrange the chamber shape and absorber to minimize residual reflections over some limited volume of space within the chamber. This volume of space is called the quiet zone. With this type of chamber design the transmit/receiver antenna is always located at the same place and the model is always placed within the quiet zone. While this practice is effective for much antenna testing, it is severely limiting for EM scattering measurements that may encounter a wide range of model sizes, a wide range of cross section levels, and requirements for bistatic as well as monostatic cross section measurements.

In the quiet zone approach to chamber design, the distance R between the transmit/receive antenna and model location within the quiet zone must remain relatively fixed. Hence, there is no opportunity to optimize R for smaller scatterers. As a result, either additional errors are introduced into the measurements because power levels at the receiver due to the scatterer are so close to the ultimate receiver sensitivity that adequate separation between the target signal and the cancelled background signals cannot be obtained, or high additional costs are incurred to provide low noise, stable power amplifiers for each frequency band. A fixed relatively large value of R easily increases the required transmitter power by 30 dB to 40 dB to preserve a given accuracy in the measured cross sections compared to the power required if R could be chosen as the minimum far field distance for a smaller scatterer. (See, for example, Eq. (28).)

3.1 Antenna/RF Components Shield

Nearly all methods of EM scattering measurements require and achieve very high cancellation of background signals. In the CW measurement method, background cancellation of -80 dB to -120 dB are typical. At these cancellation levels the equipment becomes very sensitivie to all levels of rf leakage, coupling, and reflections that normally are ignored in other types of EM measurements.

In particular, the antennas transmit some small power directly behind their reflectors, or along the waveguide or coaxial lines of horn antennas. They are also sensitive to any power emanating from the transmission line components. The antennas are, in fact, quite tightly coupled to the space immediately behind their reflectors. Any motion in this space including that of a hand near the transmission line components changes the fields in this region and especially the amount of these fields that is reflected to the antennas, thereby upsetting the background cancellation.

It is common practice for an operator to stand in this space to adjust attenuators, phase shifters, and matching devices in order to cancel the background signals. Without adequate shielding between the antennas and operator space, the final cancellation becomes a function of the position of the operator's hand, arm, or head.

If high degrees of cancellation are to be achieved and maintained during a measurement time, it is essential that sufficient shielding is provided between the antennas and operator space for an operator to approach the rf components, make adjustments, and depart without upsetting the cancellation. In effect, the antennas must become a part of the chamber only, and the operator space at the rf components must be isolated completely from the interior of the chamber.

Several options for achieving this separation of the antennas and the transmission line, rf power sources, and receiver are sketched in Figure 4. One additional restraint is that the transmission line connecting the principal transmission/components assembly and the antennas should be kept as short as possible. Hence, for higher frequency assemblies, it may be advantageous to include provision for using thinner absorber immediately behind the transmit/receive antennas.

From the view of operational convenience the most attractive arrangement is shown in Figure 4a. It is a full wall with direct access to the chamber, the main building corridor, and the equipment and storage room. In the arrangement of Figure 4a as well as that of Figure 4c, the rf equipment space could be shielded at reasonable cost and this would be desirable. The partial wall shown in Figure 4b will afford somewhat less effective shielding of the operator space but if the wall is quite large compared to the antennas this arrangement should provide adequate separation of the spaces.

In general, the actual arrangement will be largely dictated by the particular space available and the existing building structure so that Figure 4 is intended to provide some guidance in points to consider both in obtaining adequate separation of the spaces and in providing operational ease.

For removal and installation of measurement setups at different frequencies small removable sections that fit within the shielding are very convenient and a design for such sections is outlined in the next section.

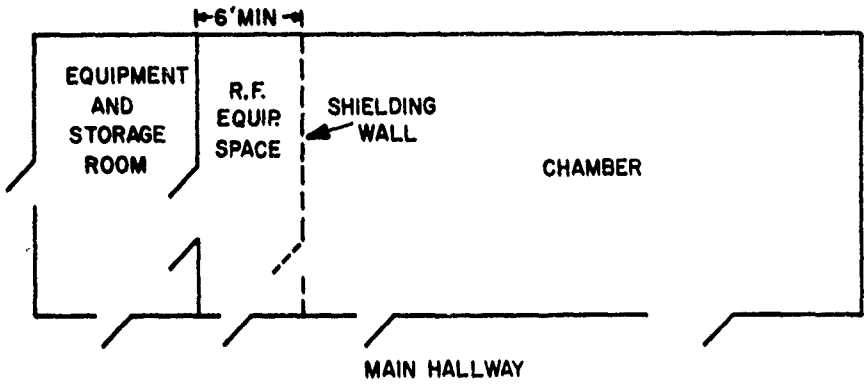

a. Full Shielding Wall

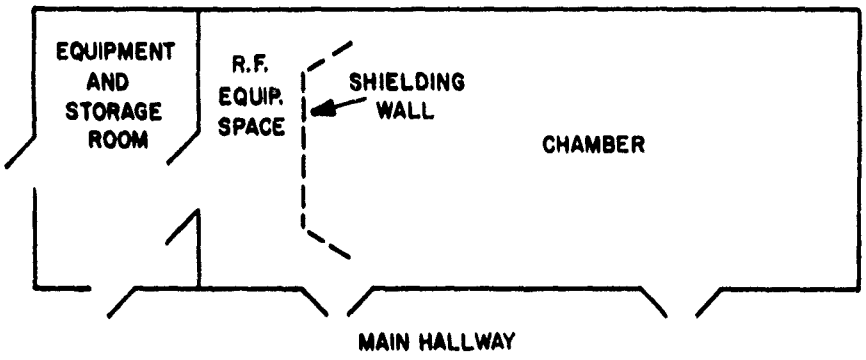

b. Partial Shielding Wall

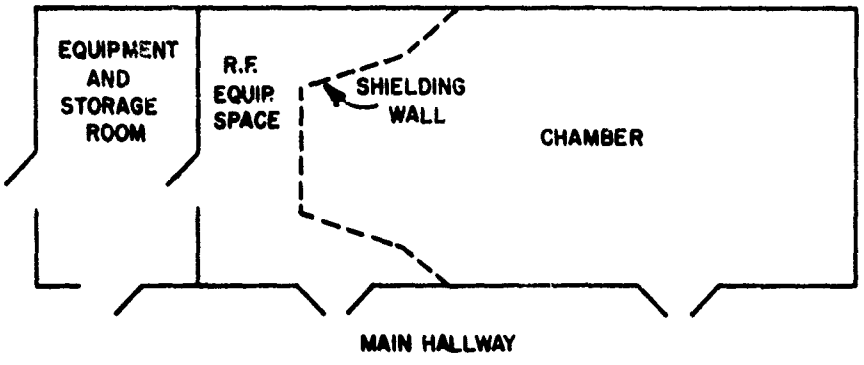

c. Tapered Shielding Wall

Figure 4. Antenna/RF Equipment Shielding Options

3.2 Removable Access Ports for Shielding Wall

This subsection outlines a relatively simple but sturdy design for removable access ports in the shielding wall. Inclusion of an array of removable, interchangeable access ports in the original chamber planning will greatly facilitate setting up experiments in the future. The design that is outlined has proven effective in use.

This basic port design consists of a piece of plywood nailed and glued to the narrow side of 2 × 4's that form the frame. The frame is flush or slightly larger than the plywood. Corners of the frame should be nailed and glued. The plywood should be at least 5/8 in. thick and 3/4 in. or thicker would be preferable. Adjacent ports are bolted together with the wide sides of the 2 × 4's frames mating. Tolerances must be held closely for the pieces to be interchangeable and removable. To facilitate removal, mating sides of the frame should be sanded smooth and finished with a hard nontacky finish. Several extra ports are useful so that antennas for each frequency band can be fitted to their own supporting port. Sufficient removable sections to completely fill the port space should be covered on the chamber side with the chamber absorber so that experiments can be set up in the chamber with no reflections from antennas on the working ports.

An array of removable sections that should be adequate for a full shielding wall is shown in Figure 5a. An optional additional port at the lower right is indicated by the dashed line. The inclusion of this additional section permits a large area to be opened in case large equipment needs to be moved into the rf equipment space. Note that the wall surrounding the removable sections must also contain the 2 × 4 framing, nailed and glued to the plywood of the wall. The removable sections are also bolted to this framing.

Figure 5b shows such an array of removable sections for the tapered chamber end. Details of the framing are shown in Figure 6. As suggested by Figure 6, the 4 × 4 ft sections are large and may be inconvenient for smaller antennas. Hence, smaller removable sections can be provided within these larger sections.

3.3 Chamber Reflections

Serious reflections within a microwave anechoic chamber all originate from the transmitting antenna either through its main beam or side lobes. There are three classes of serious reflections within a chamber. Each class introduces somewhat different errors and each class is susceptible to different cures.

The first class of reflections is comprised of energy reflected from the walls, floor, and ceiling that passes through the space to be occupied by the model, the model space. If these reflections are sufficiently strong so that the reflected fields on the model space have an amplitude that is significant compared to the amplitude of the direct radiation, an interference pattern is created over the model

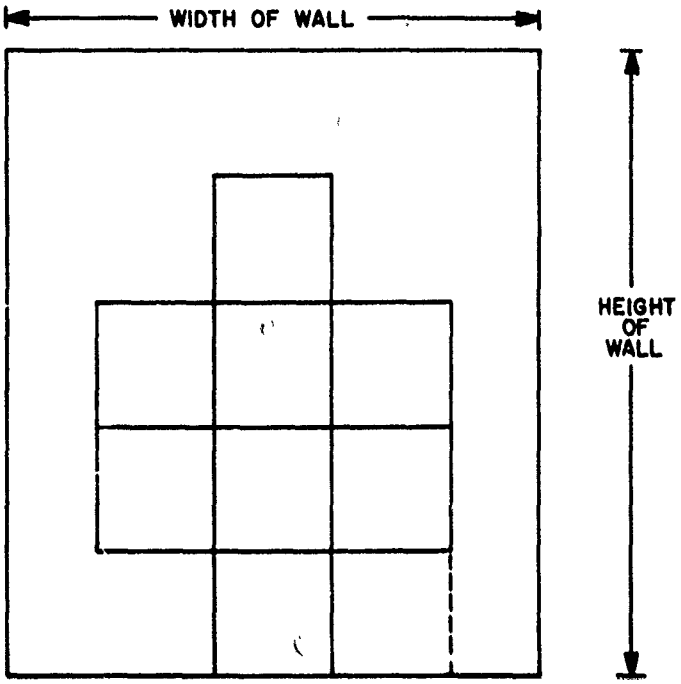

Figure 5a. Port Arrangement of Full Wall Shielding. Dashed section indicates optional additional port for access to RF equipment space for large equipment

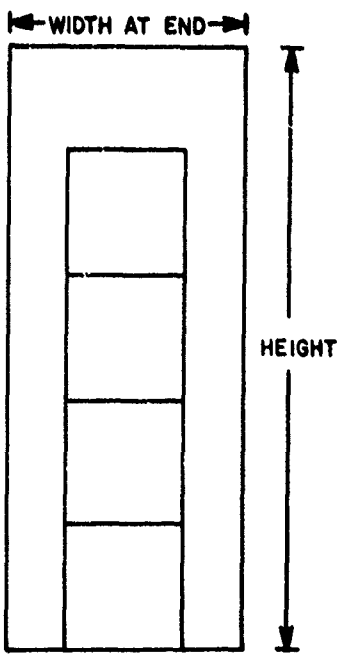

Figure 5b. Port Arrangement for Tapered Chamber

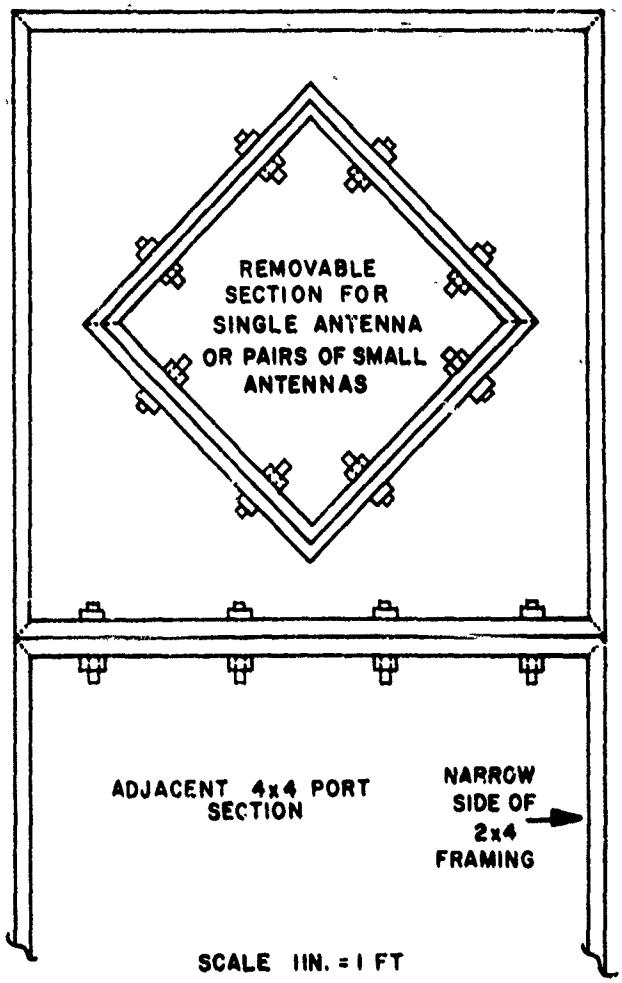

Figure 6. Details of Port Sections

space. This negates an otherwise accurate approximation to a planewave field over the model space. These reflections are, in effect, multipath problems. The quiet zone approach to chamber design is aimed primarily at reducing these reflections. These reflections arise most frequently from a transmitting antenna with a main beam that is wider than necessary, or from the first few side lobes of the transmitter beam.

If reflections from the walls and ceilings were specular, the important reflecting regions of the walls and ceiling would be from the transmit/receive antenna to

a point approximately midway of the chamber. This corresponds to incidence angles at the walls from about 90° to an angle θ given by:

$$\theta = 57.3 \tan^{-1} R/\ell \qquad (33)$$

where ℓ is the total width of the room and R is the antenna to scatterer distance. Assuming as an illustrative example an effective finished room length of about 10 m with widths of 18 ft = 5.49 m yields

$$\theta = 57.3 \tan^{-1} 10/5.49 = 61.2^{\circ} \quad .$$

Since scattering from the absorber-covered wall will be largely diffuse, important reflections will occur out to perhaps 75°.

A second class of reflections are potentially more serious for scattering measurements. This class is comprised of those reflections that come from walls, floor, and ceiling directly back to the receiving antenna. These reflections frequently are a significant part of the background signal that must be canceled in a CW system; the larger such reflections are, the more difficult it is to maintain cancellation of the background signals during a measurement. The more serious of these reflections occur through the far out side lobes of the antenna and therefore come from reflecting obstacles that are located physically close to the antenna so that little relief is provided by 1/R spatial attenuation. Since such reflections may be a significant part of the background signal that must be canceled in CW measurement systems, the structures giving rise to these reflections must be particularly rigid and free from vibrations or other short term motions. Even minute movements will upset low cancellation levels of the background signals and thereby limit the measurement accuracy. It is to reduce the effects of such reflections that tunnel antennas are highly recommended for radar scattering measurements. The use of antenna tunnels readily reduce far out side lobes by 15 to 20 dB and, therefore, the net sensitivity of a system to such reflections by 30 dB to 40 dB. The reflectors used with reflector antennas for indoor scattering measurements tend to be relatively small, accentuating spillover from conventional feeds. An alternative antenna might be some form of the Bell horn if a proper holding design could be found to permit central axis feeding. The latter is very useful because it permits ready rotation of the antenna for measurements at different polarizations.

The third kind of serious chamber reflections come from the back wall, at which the transmit/receive antenna looks, and are due to two related causes. The first is the obvious one which is that all of the transmitting beam that is not intercepted by the scatter strikes the back wall and is reflected back toward the receiver.

This can also create a standing wave over the model space as well as provide a significant contribution to the background signal. The best cure is to use high quality absorber on the back wall.

The second source of backwall reflection error is a little more subtle. It is due to forward scattering by the scatterer under investigation. The forward scatter of an object is generally much larger than the backscatter, and this concentrated beam strikes the backwall directly in line with the transmit/receive antenna and scattering model. For a sphere in the optics region of scattering,[5] for example

$$\sigma_{forward} = (ka)^2(\pi a)^2 \tag{33a}$$

$$\sigma_{back} = (\pi a^2) \tag{33b}$$

resulting in such forward to backscatter ratios as given in Table 4.

Table 4. Forward Scatter to Backscatter Ratios for a Sphere

$\sigma_r = \frac{\sigma(180^o)}{\sigma(0^o)} = (ka)^2$			
Sphere Size (ka)	σ_r (dB)	Sphere Size (ka)	σ_r (dB)
3.0	9.5	15.0	23.5
5.0	14.0	20.0	26.0
7.5	17.5	25.0	28.0
10.0	20.0	30.0	29.5

This energy strikes the back wall and is partially reflected to the model where it is again enhanced by forward scattering and returned to the transmit/receive antenna, resulting in an error signal that can be relatively large under adverse chamber arrangements and which is difficult to separate from the true signal that is backscattered from the model.

---

5. Van De Hulst, H.C. (1957) Light Scattering by Small Particles, John Wiley & Sons, Inc., New York, Chapt. 9.

The following analysis of signal strength at the receiving antenna due to the forward scattered signal is approximate, but provides a simple estimate of errors from this source.

3.4 Reflections from Back Wall

Three distinct properties of reflections from the back wall can have serious effects on measurements of scattered fields, and the three will be examined individually in this section. The properties of concern are the amount of power reflected to the receiving antenna with no scatter present, the field distortion caused over the model space by backwall reflections, and the power returned to the receiver from the back wall by way of forward scattering of the model.

3.4.1 POWER REFLECTED TO THE RECEIVER WITH NO SCATTERER PRESENT

From Figure 7, the power density from the transmitter incidence on the backwall is

$$P_i = \frac{P_t G_t}{4\pi(R_1 + R_2)^2} \qquad \text{(power incident on back wall)} \tag{34a}$$

where P_t is the total transmitter power radiated by the antenna, G_t is the gain of the antenna, R_1 is the distance from the transmit/receive antenna to the center of the space to be occupied by the model, and R_2 is the distance from the center of the model space to the backwall. Let the area of the backwall that is illuminated by the incident beam be assumed to be elliptical. Then the axes of the ellipse are given by $(R_1 + R_2)\theta_A$ and $(R_1 + R_2)\phi_B$ where θ_A and ϕ_B are the elevation and azimuth beamwidths of the antenna. Generally, half power beam angles provide sufficient accuracy but 1/10 beam angles may be used for better results. The area of the wall that is illuminated is

$$\text{(wall area illuminated)} = \frac{\pi}{4}(R_1 + R_2)^2\,\theta_A \phi_B \ . \tag{34b}$$

Power reflected by the wall to the receiving antenna is

$$P_{rw} = \frac{P_t G_t}{(4\pi)^2 (R_1 + R_2)^4} \cdot \frac{\pi}{4}(R_1 + R_2)^2\,\theta_A \phi_B \Gamma_w$$

$$= \frac{P_t G_t}{16(4\pi)(R_1 + R_2)^2}\,\theta_A \phi_B \Gamma_w \qquad \text{(power density at transmit/receive antenna from back wall)} \tag{34c}$$

where Γ_w is the power reflection coefficient per unit area of the wall. The power absorbed by the antenna is

$$P_r = \frac{P_t G^2 \lambda^2}{16(4\pi)^2 (R_1 + R_2)^2} \theta_A \phi_B \Gamma_w \quad , \tag{34d}$$

and

$$\frac{P_r}{P_t} = \frac{G^2 \lambda^2}{16(4\pi)^2 (R_1 + R_2)^2} \theta_A \phi_B \Gamma_w \quad . \quad \text{(received power from back wall, no scatterer)} \tag{34e}$$

Note the $1/R^2$ behavior that is a direct consequence of the wall's acting as an extended scatterer instead of a point scatterer.

Reflections of this kind from the back wall are one of the principal coupling mechanisms between the transmitting and receiving paths of a cw cancellation scattering measurement systems, and the power described by Eq. (34e) is a principal component of the background and leakage signal that must be canceled or reduced. To obtain a feeling for the magnitudes involved in Eq. (34e) consider the following example, namely a chamber with a total working length of $(R_1 + R_2) =$ 10 m be used for measurements at 3 GHz ($\lambda = 0.1$ m). Let the transmit/receive antenna be circular and the largest one for which the conventional far field criterion can be satisfied in the chamber. Thus,

$$R_1 + R_2 = 2D^2/\lambda \quad , \quad D = \sqrt{\frac{(R_1 + R_2)\lambda}{2}} = 0.707 \text{ m} \quad .$$

Also, let the antenna be 60 percent efficient. As will be shown subsequently, $G = 0.3\pi^2 (R_1 + R_2)/\lambda$. For simplicity, let the beamwidths be equal and given by $\theta_A = \phi_B = \lambda/D$. Eq. (34e) becomes

$$\frac{P_r}{P_t} = \frac{0.9\pi^4 (R_1 + R_2)^2 \lambda^2}{16(4\pi)^2 (R_1 + R_2)^2 \lambda^2} \cdot \left(\frac{\lambda}{D}\right)^2 \Gamma_w \tag{34f}$$

$$= \left(\frac{0.3\pi}{16}\right)^2 \left(\frac{\lambda}{D}\right)^2 \Gamma_w \tag{34g}$$

$$\frac{P_r}{P_t} = \left(\frac{0.3\pi}{16}\right)^2 \left(\frac{10^{-1}}{5}\right) \Gamma_w = 6.94(10^{-4})\Gamma_w \quad . \tag{34h}$$

If 40 dB absorber is used on the backwall, then $P_r/P_t = 6.94(10^{-8})$; for 20 dB absorber the result is $6.94(10^{-6})$. It is interesting to compare this result to the power returned by a sphere of ka = 20 placed at R_1 = 8 m and also measured at f = 3 GHz with the same antenna. Inserting the appropriate numbers in Eq. (32) yields $P_r/P_t = 3.43(10^{-5})$. Hence, power received from the wall covered with 40 dB absorber would not contribute significant error to measurement of a ka = 20 sphere with no additional cancellation; however, if 20 dB absorber were used at least 10 dB of cancellation would be required to insure no more than ±1 dB error in the measured results.

3.4.2 FIELDS OVER THE MODEL SPACE, NO SCATTERER

The incident power density at the model space due to the direct wave from the transmitting antenna is given by Eq. (34a) with $(R_1 + R_2)$ replaced by R_1. The power density due to reflections from the back wall is given by Eq. (34c) with $(R_1 + R_2)$ replaced by R_2. These fields are traveling in opposite directions and produce an interference pattern over the model space with a standing wave ratio (SWR) given by

$$SWR_m = \frac{\sqrt{\frac{P_t G_t}{4\pi R_1^2}} + \sqrt{\frac{P_t G_t \theta_A \phi_B \Gamma_w}{16(4\pi)R_2^2}}}{\sqrt{\frac{P_t G_t}{4\pi R_1^2}} - \sqrt{\frac{P_t G_t \theta_A \phi_B \Gamma_w}{16(4\pi)R_2^2}}} \tag{34i}$$

or

$$SWR_m = \frac{1 + 1/4(R_1/R_2)\sqrt{\theta_A \phi_B \Gamma_w}}{1 - 1/4(R_1/R_2)\ \phi_B\ \theta_A \Gamma_w} \tag{34j}$$

where variations of $1/R^2$ over the model space have been ignored and a subscript on SWR is added to designate the model space. Equations (34j) and (34c) assume the point where the power is to be determined to be in the far field of the illuminated area of the wall. The most common situation occurs with the model space very close to the wall. For this case a more accurate model is obtained simply by ignoring the spherical spreading and assuming the wave from the wall to be reflected to the model space simply as a planewave. In this case,

$$SWR_m \doteq \frac{1+\sqrt{\Gamma_w}}{1-\sqrt{\Gamma_w}} \quad . \tag{34k}$$

In this case, if 40 dB absorber is used $\Gamma_w = 10^{-4}$ and $\sqrt{\Gamma_w} = 10^{-2}$ so that $SWR_m = 1.01 = 0.17$ dB. If 20 dB absorber were used, $\Gamma_w = 10^{-2}$ and $SWR_m = 1.222 = 1.74$ dB.

3.4.3 POWER AT RECEIVING ANTENNA DUE TO FORWARD SCATTERING BY MODEL

Let a scattering model be located in the model space at a distance R_1 from the transmit/receive antenna, and a distance R_2 from the wall (Figure 7). The power density from the transmitter is given by Eq. (34a) with R_1 replacing $(R_1 + R_2)$. The power returned from the model directly to the receiving antenna is

$$\left(\begin{array}{l}\text{power density at antenna}\\ \text{from model backscatter}\end{array}\right) = \frac{P_t G_t \sigma_B}{(4\pi)^2 R_1^2} \tag{35a}$$

where σ_B designates backscatter cross section. The power density at the wall due to forward scatter of the model is

$$\left(\begin{array}{l}\text{power density at wall}\\ \text{due to forward scatter}\end{array}\right) = \frac{P_t G_t \sigma_F}{(4\pi)^2 R_1^2 R_2^2} \quad . \tag{35b}$$

Again, since the model may be quite close to the wall and hence not in the far field of that patch of the wall that is illuminated by the forward scatter lobe of the mode, simple plane wave reflection is assumed. Hence, the power density at the model due to reflection of the forward scatter by the wall is

$$\left(\begin{array}{l}\text{power density at model}\\ \text{after reflection from wall}\end{array}\right) = \frac{P_t G_t \sigma_F}{(4\pi)^2 R_1^2 R_2^2} \Gamma_w \quad . \tag{35c}$$

This wave again undergoes forward scattering, this time toward the receiving antenna. The power density at the receiving antenna due to this source is

$$\left(\begin{array}{l}\text{power density at antenna}\\ \text{due to forward scattering}\end{array}\right) = \frac{P_t G_t \sigma_F^2 \Gamma_w}{(4\pi)^3 R_1^4 R_2^2} \quad . \tag{35d}$$

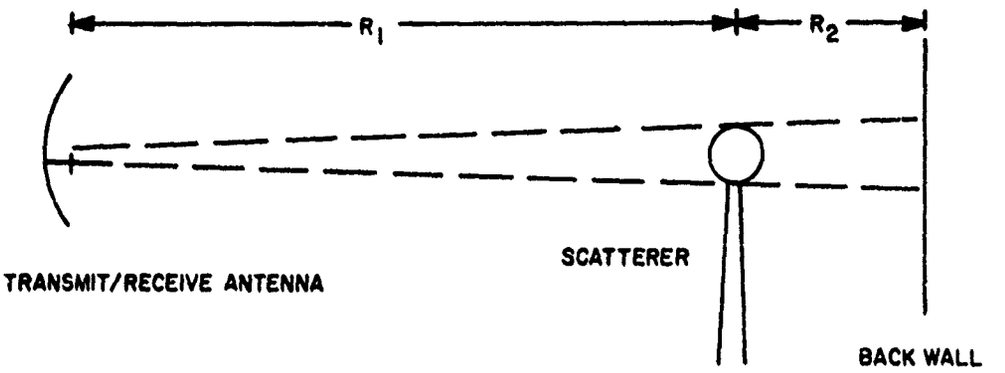

Figure 7. Geometry Illustrating Forward Scattering

The ratio P_r of this power density to the desired power density from the model backscatter is

$$P_r = \frac{P_t G_t {}^2_F \Gamma_w}{(4\pi)^3 R_1^4 R_2^2} \cdot \frac{(4\pi)^2 R_1^4}{P_t G_t \sigma_B} = \frac{\sigma_F^2}{\sigma_B} \frac{\Gamma_w}{4\pi R_2^2} \tag{35e}$$

As an example, consider the scattering model to be a sphere of ka = 20 located at R_2 = 1 m from the wall. From table 4, $\sigma_F = 400\sigma_B$ and if the measurements are to be made at 3 GHz, $\sigma_B = 1/\pi$. Therefore,

$$P_r = \frac{1600\ \sigma_B}{4\pi} \Gamma_w = \frac{1600}{4\pi^2} \Gamma_w = 40.53\ \Gamma_w$$

For this example, 30 dB absorber would be sufficient to insure errors from this source to be no larger than ±1 dB. For a more general scatterer, that may have higher ratios of σ_F to σ_B even 40 dB absorber may be marginal. The importance of measuring the model at minimum values of R_2 is clear from Eq. (35e). Also, the desirability of using the best possible absorber near the center of the back wall where illumination by forward scatter is strongest is clear.

Two methods of minimizing errors due to reflections from the wall are contained in Eq. (35e). They are to reduce Γ_w and increase R_2. An additional method that is also related to reducing Γ_w has been used with varying reported degrees of success.

This method is to tilt the back wall so that the reflected energy misses the model and antenna. In effect a null of the scattering pattern of the wall is directed

along the central axis of the experiment. In fact, the success of this method depends on the reflection from the back wall being largely specular instead of diffuse. The additional cost of including a tilting wall will be substantial because a movable wall must have an independent supporting structure that is absolutely rigid and vibration free, and the wall must have a mechanism for precisely controlling its motion. Any vibrations introduced by the wall will limit cancellation levels that can be maintained and the reduced cancellation levels that can be maintained can easily introduce error limitations that outweigh reduced back wall reflections. Also, the movable wall will not be useful for measurements that are to be made over a program controlled set of frequencies.

A much cheaper alternative to the movable wall is to preserve the capability of measurements with the experimental axis skewed with respect to the longitudinal axis of the chamber, this is, with the model placed to one side of the other of the center of the chamber.

3.5 Estimated Interference from Multipath Signals

This section contains a zeroth order approximate estimate of the maximum strength to be expected at the central axis of the chamber from signals that are reflected from the walls, floor, and ceiling, and traverse the model space.

The estimate can be made quite accurate by using bistatic scattering pattern of the actual absorber chosen, and by using the actual antenna patterns at the frequency of interest; the basic technique will be the same as used herein.

The appropriate geometry is sketched in Figure 8 where R is the direct distance from antenna to model, the wall-to-wall chamber width is w, the antenna pattern angle is ϕ, and the angle at which offending rays strike the absorber is θ. Because of Snell's Law, the most prominent offending reflections will always occur at points along the wall midway between the antenna and model, even when account is taken of the actual diffuse nature of scattering by the absorber. For simplicity, it is assumed that reflections take place from the base of the absorber.

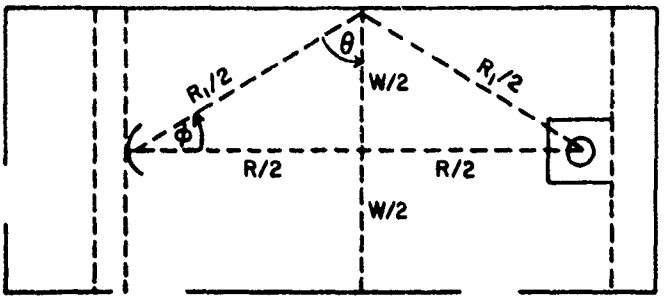

Figure 8. Geometry for Estimating Multipath Reflections

If E_o is the maximum field just in front of the antenna, the direct field at the model space is

$$E_{mo} = E_o/R \quad . \tag{36}$$

The reflected field at the model is approximately

$$E_{ml} = \frac{\alpha_s \alpha_a E_o}{R_1} \tag{37}$$

where α_s is the ratio of the antenna field in direction ϕ to the field in the direction of the main beam; α_a is the reflection coefficient of the absorber at angle θ; and R_1 is twice the distance from the antenna to the point of reflection, the distance traveled by the reflected ray. The ratio of the fields at the model is

$$E_R = E_{ml}/E_o = \alpha_s \alpha_a R/R_1 \quad . \tag{38}$$

From Figure 8

$$R_1 = R\sqrt{1 + (w/R)^2} \tag{39}$$

$$\phi = (57.3 \tan^{-1} w/R)^o \tag{40}$$

$$\theta = 90^o - (57.3 \tan^{-1} w/R)^o \tag{41}$$

Therefore

$$R/R_1 = \frac{1}{\sqrt{1 + (w/R)^2}} \tag{42}$$

and

$$E_R = \frac{\alpha_s \alpha_a}{\sqrt{1 + (w/R)^2}} \tag{43}$$

In dB

$$E_{RdB} = \alpha_{sdB} + \alpha_{adB} - 20 \log \sqrt{1 + (w/R)^2} \tag{44}$$

where α_{sdB} is simply the value in dB of the antenna pattern at angle ϕ and α_{adB} is the absorber reflection coefficient in dB at angle $\theta = 90^{o} - \phi$.

The theoretical pattern of a circular antenna with uniform illumination is given by Eq. (13). In dB,

$$\alpha_s = 20 \log E_{TC} = 20 \log \left[\frac{J_1(\pi D/\lambda \cdot \sin \phi)}{(\pi D/\lambda \cdot \sin \phi)}\right] . \tag{45}$$

For convenience this function is graphed in Figure 9.

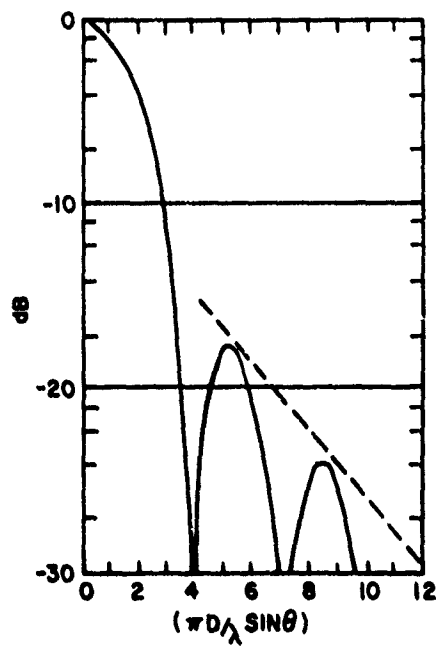

Figure 9. Theoretical Pattern-Circular Aperture Uniform Illumination

In the worst case, reflections from both walls, the ceiling, and floor would all arrive in phase at the model. In this case Eq. (43) is multiplied by 4 and Eq. (44) becomes

$$E_{RdB} = 12 + \alpha_{sdB} + \alpha_{adB} - 10 \log [1 + (w/R)^2] \tag{46}$$

As a function of R the worst case will occur when R is largest because this is when the angle ϕ corresponds to the closer-in side lobes that are higher, and when the angle of incidence on the absorber is furthest from normal.

For the following examples, R = 30 ft and w = 18 ft. The attenuator factors are taken from the following section. With these values of R and w, for all of the calculations,

$$\phi = \tan^{-1} 18/30 = 31^{\circ} \quad , \quad \sin\phi = 0.5150$$

$$\theta = 90^{\circ} - \phi = 59^{\circ}$$

$$20 \log \sqrt{1 + (w/R)^2} = 1.34 \text{ dB}$$

Equation (46) is used for the examples.

Examples:

1. $f = 1$ GHz, $D = 3$ ft

   $\frac{\pi D}{\lambda} \sin\phi = 4.85 \qquad \alpha_{sdB} = -19$ dB, $\alpha_{adB} = -25$ dB, $E_{RdB} = -33.3$ dB

2. $f = 2$ GHz, $D = 3$ ft, $\lambda = 0.492$ ft

   $\frac{\pi D}{\lambda} \sin\phi = 9.86 \qquad \alpha_{sdB} = -28$ dB, $\alpha_{adB} = -42$ dB, $E_{RdB} = -51.3$ dB

3. $f = 4$ GHz, $D = 1.5$ ft, $\lambda = 0.246$ ft

   $\frac{\pi D}{\lambda} \sin\phi = 9.86 \qquad \alpha_{sdB} = -28$ dB, $\alpha_{adB} = -42$ dB, $E_{RdB} = -59.3$ dB

4. $f = 10$ GHz, $D = 1.0$ ft, $\lambda = 0.0983$ ft

   $\frac{\pi D}{\lambda} \sin\phi = 16.46 \qquad \alpha_{sdB} = -35$ dB, $\alpha_{adB} = -48$ dB, $E_{RdB} = -72.3$ dB

Even under conditions of relatively diffuse scattering from the absorber there should be combinations of R for which ϕ is at the antenna pattern nulls and for which E_{RdB} is very low. This may be an especially important consideration for obtaining high quality results with relatively large, low cross section scatterers at frequencies near 1 GHz.

3.6 Absorber Characteristics

If the use of sophisticated chamber design for scattering measurement systems is ruled out by arguments of versatility, the remaining questions center on the choice of absorber to be used to line the floor, ceiling, and walls of the chamber. To provide a basis for these choices the characteristics of current state of the art pyramidal absorbers are briefly examined in this section.

Figure 10 shows reflectivity in dB at normal incidence as a function of absorber thickness for typical pyramidal absorber at 1 GHz. Reflectivity values are relative to the reflectivity of square metal plates and the curve is based on a composite of data from the literature of several leading manufacturers of absorber.

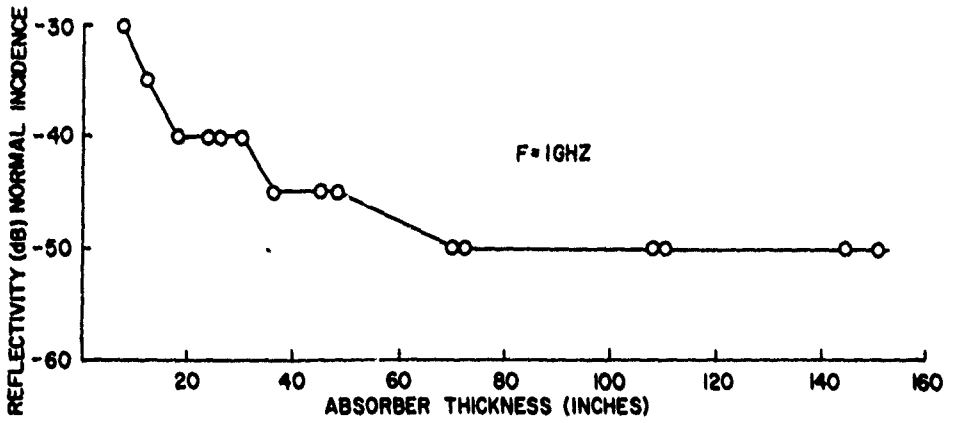

Figure 10. Pyramidal Absorber Reflectivity (Normal Incidence)

The most striking feature of Figure 10 is the large increase in thickness that is required to obtain significant reduction in reflectivity beyond -40 dB at 1 GHz. An 18 in. thickness provides a reflectivity of -40 dB at 1 GHz, but to obtain a 5 dB improvement requires 36 in. absorber and to obtain a 10 dB improvement to -50 dB requires an increase in absorber thickness to 70 in. to 72 in.

Wide angle behavior of pyramidal absorber is summarized in Figure 11 which shows reflectivity in dB as a function of absorber thickness in wavelength. Again, the curves shown are based on composite data so do not apply to anyone specific absorber but rather indicate what typically might be expected. Also, in any given situation there will probably be polarization differences in the reflectivity and these differences are not reflected in the averaged curves of Figure 11.

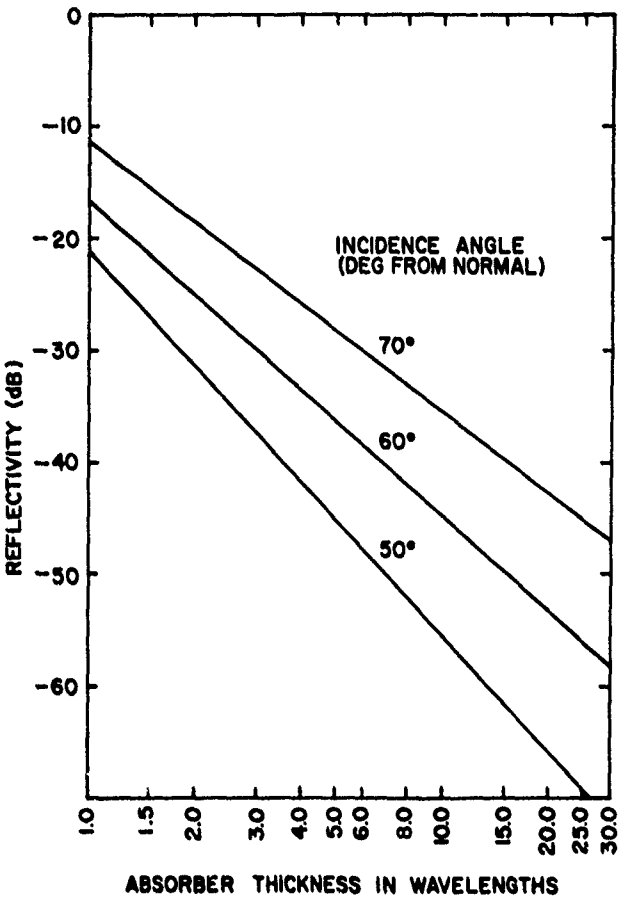

Figure 11. Wideangle Reflectivity—Pyramidal Absorber

As might be expected the greatest deterioration in reflectivity with angle occurs at lower frequencies for a given absorber thickness. Thus, the reflectivity at 1.0 GHz with 18 in. absorber changes from -40 dB at normal incidence to about -16 dB at 70° incidence.

As shown previously, serious reflections from walls and floors in a chamber of about 10 m length and 6 m width would occur at angles of incidence to about 60° and allowing for diffuse reflections, to about 70°. Based on Figure 11, the use of 24 in. absorber on the walls, ceiling, and floor would insure reflectivity no higher than -30 dB for frequencies of higher than approximately 3.0 GHz, and reflectivity of -40 dB or better for frequencies higher than approximately 7.4 GHz.

For convenience, reflection coefficients for 18, 24, and 36 in. absorber at incident angles of 0°, 50°, 60°, and 70°, for 1.0 GHz are summarized in Table 5 and typical values at normal incidences for a range of frequencies are summarized in Table 6.

Table 5. Approximate Pyramidal Absorber Reflection Coefficients at 1 GHz

Incidence Angle	Reflection Coefficients (in dB) 18 in.	24 in.	36 in.
0° (normal)	-40	-40	-45
50°	-25	-30	-40
60°	-22	-25	-30
70°	-15	-18	-22

At higher frequencies where a given absorber contains more wavelengths, reflection coefficients remain good out to even 70°. At X-band where the wavelength is approximately an inch, the reflection coefficient would be approximately -40 dB at 70°.

Table 6. Normal Incidence Frequency Behavior, Pyramidal Absorber

Absorber Thickness (in.)	Frequency Band (dB) K	K_U	X	C	S	L
18	-50	-50	-50	-50	-45	-40
24	-50	-50	-50	-50	-50	-40
36	-50	-50	-50	-50	-50	-45

There are several additional basic considerations in absorber choices. The first is that use of thick absorber with improved reflectivity levels also reduces the usable measurement space in a chamber of finite size, and by moving the walls closer to the scatter, the advantages of path length attenuation are reduced. The end result can well be no better than having a thinner absorber placed further from the scatterer.

The second consideration is that significant improvement in wide angle reflectivity might be achieved by mounting the absorber at 45° angles to the horizontal or vertical. That is, instead of aligning the standard 2×2 ft sections with their edges parallel to the walls and floor as is common practice, align them at 45° to these

surfaces. When radiation from the antenna falls on the pyramids from other than normal incidence, the energy tends to strike the flat surface of the pyramids in the usual mounting configuration. These flat surfaces are not particularly good absorbers and multiple absorbing reflections are discouraged with this orientation of the absorber. If the absorber is mounted at 45° orientation, energy incident at wide angles will tend to strike the corners of the pyramids and be absorbed by additional multiple reflections between the pyramids.

4. TRANSMIT/RECEIVE ANTENNAS

The gain of a reflector type of antenna is given by[4] (Chap. 7)

$$G = \frac{4\pi A_e}{\lambda} \tag{47}$$

where A_e is the effective area of the reflector and λ is the wavelength. Typically, reflector antennas are about 60 percent efficient because of spillover from the feeds and power tapers across the apertures to improve side lobes. Assuming 60 percent efficiency,

$$G = \frac{4\pi(0.6)A}{\lambda^2} \tag{48}$$

where A is the physical area of the reflector. For a circular reflector of diameter D,

$$A = \frac{\pi D^2}{\lambda} \tag{49}$$

and the gain becomes

$$G = 0.6\pi^2(D/\lambda)^2 \quad \text{(circular antenna 60 percent efficient)} \; . \tag{50}$$

The antenna far field is given by the same relation as the conventional scattering far field,

$$R = 2D^2/\lambda \tag{51}$$

Based on the conventional far field criterion, the largest antenna that can be utilized over a range R is, from Eq. (51)

$$D = \sqrt{\frac{R\lambda}{2}} \quad . \tag{52}$$

Inserting this value of D into Eq. (50) yields

$$G = 0.3\pi^2(R/\lambda) \quad . \tag{53}$$

The point is that if the antenna must be a distance R from a scattering model to measure in the far field of the model, the largest antenna that can be used, subject to the usual far field criterion, is given by Eq. (52) and has a gain given by Eq. (53) or Eq. (50).

Since the far field criterion of the antenna and the scatterer are the same, it follows that the antenna defined by Eq. (52) is equal in size to the scattering model.

An antenna equal in size to the scattering model is also an optimum antenna to be used for scattering measurements under conventional far field criteria. The reason is that if a larger antenna were chosen, R must be increased beyond the minimum required by the model and the received power, Eq. (25), will be reduced by a factor of k^4 where the far field distance, R, required by the larger antenna is given $R_1 = kR$. If a smaller antenna is used, the receiver power will be reduced through the G^2 term by a factor of k^2 where the smaller antenna is related to the optimum only by $D_1 = kD$ because R in this case is determined by the model and cannot be reduced by use of the smaller antenna. The optimum antenna, equal in size to the scatterer, in effect minimizes R, the most sensitive term in the power relation.

Equation (19) shows that for a uniformly illuminated circular reflector antenna having a diameter D equal to the maximum model dimension L, the lateral distance between half power points of the beam in $\ell = 2$ L, twice the model's maximum dimension. With the aid of Eq. (15) it is easy to show that for a model perfectly centered in the antenna beam so that it extends between $\ell = \pm\frac{x}{4}$ where $x = \mu D\theta/\lambda$, the incident field will be down by -0.71 dB at the ends of the model for a total variation over the model of ±0.35 dB.

An expanded graph showing the first 3 dB region of the pattern of the uniformly illuminated aperture of Figure 9 is shown in Figure 12 to illustrate the field variation to be expected in the central region of the beam. In effect, Figure 12 defines the accuracy with which a model must be located within the beam. For example, for a variation no greater than ±1/2 dB of field over the model space, the model must be included in a region of approximately ±0.6 D of the center of the beam. Similarly, for the field to be constant within ±1 dB, the model must be within ±0.84 D of the beam center.

The following comments apply to an antenna with uniform illumination.

If an antenna is used with D larger than the optimum by $\sqrt{2}$ and the same range distance R is retained, the lateral distance between the half power points is $\sqrt{2}$ L; if the antenna were taken to be twice the optimum, the half power distance at the model space would be just equal to L, resulting in a field variation of 3 dB over a perfectly centered model.

Any taper across the antenna aperture will result in wide beams and hence, in larger 3 dB distances.

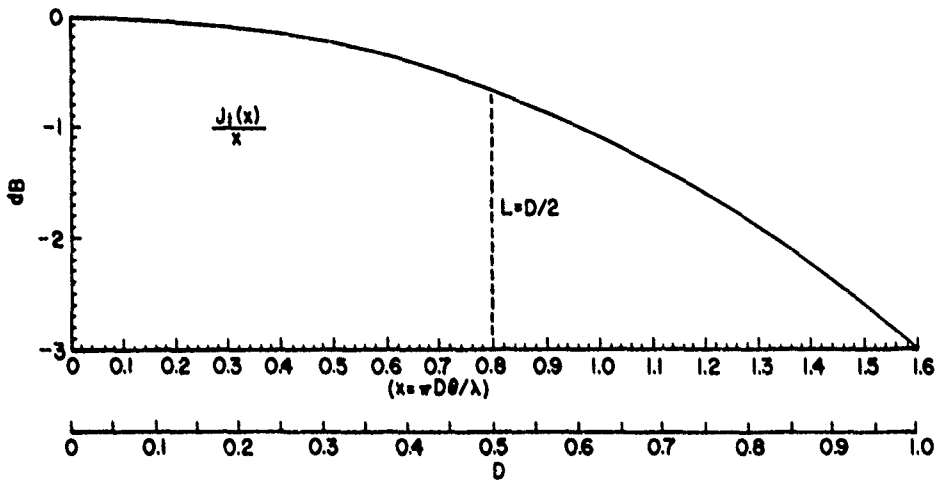

Figure 12. Lateral Field Variation at $R = 2D^2/\lambda$

4.1 Practical Approximations to the Optimum Antenna

The use of an optimum or even near optimum antenna for each scatterer to be measured implies the ready availability of a large selection of single or pairs of antenna assemblies, and this is usually not practical from a cost point of view. The antennas for scattering measurements must be as rigid and vibration-free as possible which means they are high quality antennas with high quality feed and antenna mounting assemblies; hence, they are expensive. In addition, there is a limited number of reflector sizes that are commercially available within the appropriate range of sizes.

The typical situation at a scattering measurement facility is that a limited set of antennas is available and that measurements of all models must be carried out with this limited set. The purpose of this section is to illustrate the salient compromises that result from the typical situation.

Consider a facility operating from 1 GHz to 40 GHz with a chamber having a maximum usable range of R = 32 ft and focus attention on maximum model sizes that can be handled. Let the optimum antenna be approximated by three sets of reflector antennas having diameters of 36, 18, and 12 in. respectively. These three antenna approximation to the ideal is shown in Figure 13 over the 1 to 40 GHz frequency band. Note that the curve for the optimum antenna of Figure 13 is also the curve for the largest model that can be used with a variation of no more than ±0.35 dB in the incident field over the model.

The principal question is how the use of a limited set of antennas of fixed size affects the lateral working distance at the model space, in this example, at a measurement distance of R = 32 ft. Assuming circular apertures with uniform illumination, half power beamwidths are given by Eq. (19a) which becomes

$$\ell = R/(fD) \tag{54a}$$

with lengths and distances in ft and frequency f in GHz. For the present example

$$\ell = 32/(fD) \quad . \tag{54b}$$

For the optimum antenna $\ell = 2D$ as shown by Eq. (19b).

Lateral half power distances calculated from Eq. (54b) for the three antennas of 36, 18, and 12 in., diameters and for the optimum antenna are shown in Figure 14.

In general it is advantageous to choose matched antenna and feed sets so that the feeds for various frequency ranges can be easily used in any of the reflectors. Thus, for example, the smaller antennas are useful at lower frequencies for smaller scattering models that can be measured at shorter ranges. Again it is emphasized that the antenna reflector, the feed, and the mounting arrangement should be absolutely rigid and vibration free. Although the above discussion has been in terms of reflector antennas, lens antenna, and horn lens combinations are also very useful for scattering measurements. The results as outlined generally apply to these types as well. Once specific antennas have been chosen the actual beamwidths of the chosen antennas can be utilized to construct a graph such as Figure 14.

A properly designed set of reflectors and feeds offers the possibility of varying the focus, and this feature can sometimes be quite useful. For example, defocusing will result in a wider beam and hence a larger region with less field variation over the model space. Similarly, for small models with low cross sections, focusing the larger antennas at short measuring ranges in their near fields can sometimes be advantageous by increasing the field concentration over the model space.

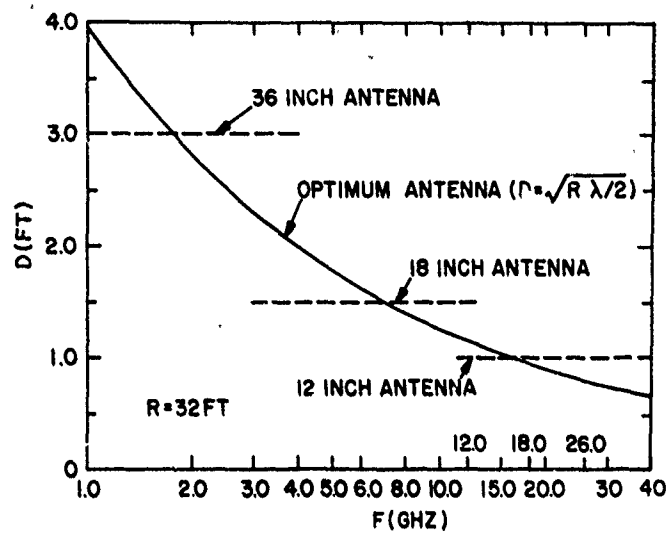

Figure 13. Three Antenna Approximation to Optimum

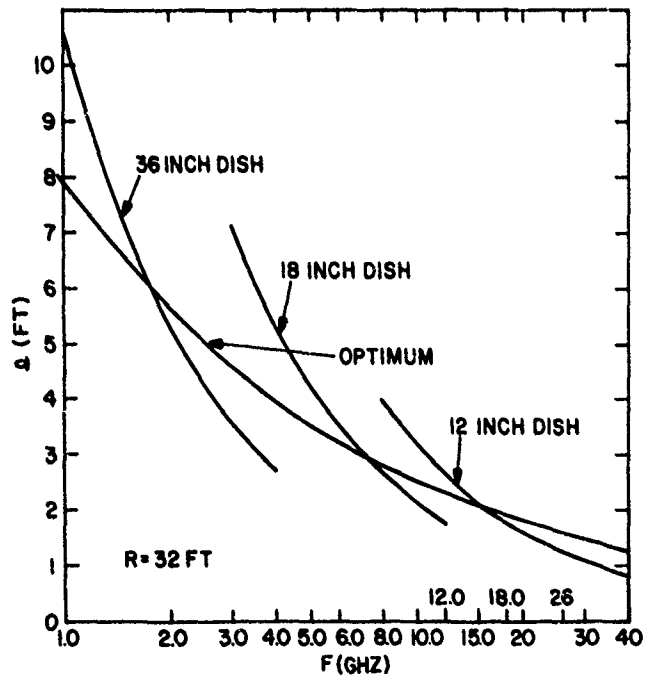

Figure 14. Half Power Distances at Model Space for Three Antenna Approximation to Optimum (Uniform Illumination, R = 32 ft)

4.2 Tunnel Antennas

Significant improvement in the performance of all of the smaller antennas can be achieved by fitting them with tunnels, and it is recommended that this be done. The tunnels should be electromagnetically sealed at the rear, either to the rim or rear of the reflector or, in case of centrally fed antennas, to the waveguide feed. The principal effect of the tunnel is to reduce spillover. Thus, the use of a tunnel significantly improves ability to maintain background cancellation. The reason is that the spillover energy corresponds to far out side lobes in the far field antenna pattern. These far out side lobes extend to 90° and frequently further from the main beam direction. When the antenna is used for scattering measurements, this energy in the far out directions strikes nearby objects and is at best partially reflected back to the antenna. Since these reflecting objects are nearby, the 1/R losses are small compared to those from the scatterer under investigation. The antenna is therefore tightly coupled to these nearby objects through its far out side lobes and the slightest movement of these scatterers relative to the antenna destroys the background cancellation. Reduction of the far out side lobes reduces the importance of nearby reflections to the balance.

A cheap method of constructing antenna tunnels for small round antennas consists of using thin absorber of the AN/75 family and purchasing sections of chimney or vent pipe equal in diameter to the reflector diameter plus twice the absorber thickness. The absorber and reflector are then fitted inside the pipe. The reflector can be held in place by screws or longer bolts passing through the pipe and the rim of the reflector. The pipe can be sealed at the rear with heavy duty aluminum foil and conducting aluminum tape. Interior supports for the aluminum foil, or a metal cover that is stiffer than the aluminum foil is recommended. The distance that the tunnel extends beyond the antenna face depends on the diameter of the antenna and the particular absorber that is used, and is best determined experimentally because the actual extension chosen usually represents a compromise between reduction of the far out radiation and slight decreases of gain and slight beam broadening that also occur. Typical useful extensions have been found to be approximately 7 to 8 in. for a 12 in. dish diameter and 4 to 5 in. for a 6 in. dish diameter at 10 GHz.

Typical results of using a tunnel of the type described above with a 6 in. dish and double dipole feed at 10 GHz are shown in Figure 15 for the tunnel extending about 4 in. beyond the reflector face. For the H-Plane patterns that are shown, this extension results in approximately a 1 dB loss of gain and an increase of approximately 25 percent in the 3 dB beamwidth but significantly reduces all radiation at angles greater than approximately $\pm 60^{\circ}$ from the main beam.

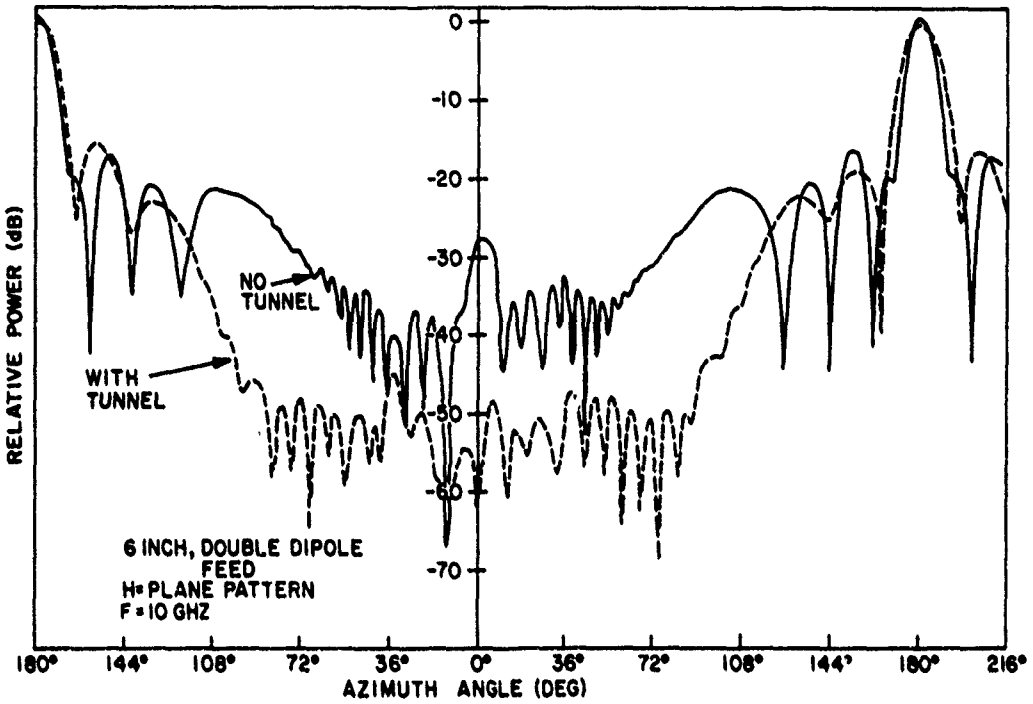

Figure 15. Results of Using Tunnel to Reduce Far Out Radiation (H-plane pattern, 6 in. reflector with double dipole feed, f = 10 GHz)

5. MODEL SUPPORT STRUCTURES

The model support structure consists of three parts: the mount, the polyfoam column, and the mounting saddle. Model supports other than polyfoam columns are used,[6] particularly for very heavy or very small models, but polyfoam columns are so common and convenient that the present discussion will be confined to them. A typical model support structure as it might be used for radar scattering measurements is shown in Figure 16.

In order to accommodate a wide variety of model sizes and weights conveniently as well as experiments at widely differing frequencies, a multisection column with interchangeable sections is suggested by Figure 16. For example, a 4 ft model for 1 GHz measurements might easily weight 100 lb and require measurement at the chamber center height of 9 to 11 ft, whereas a 4 in. model for measurement at 10 GHz to 40 GHz is more likely to weigh less than 1 lb and be more conveniently

6. Freeny, C.C. (1966) Target support parameters associated with radar reflectivity measurements, Proc. IEEE 53:929-936.

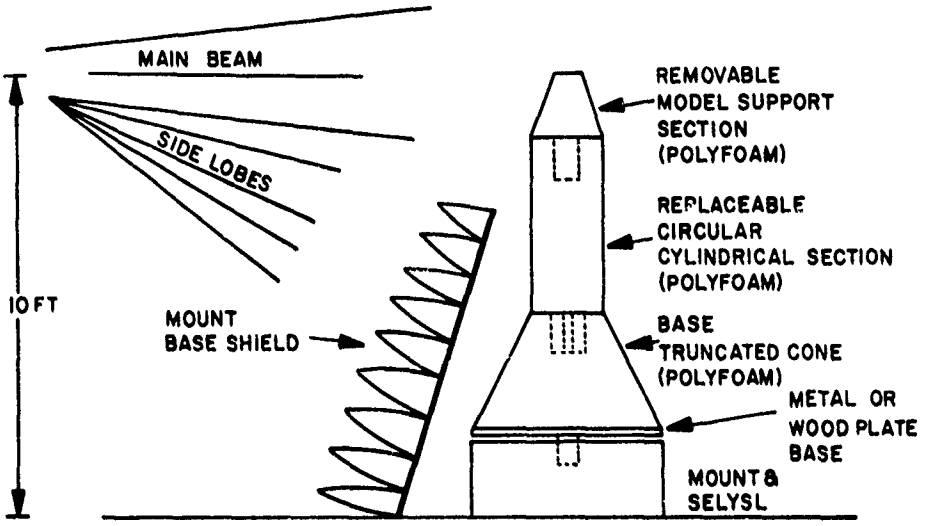

Figure 16. Typical Model Support Structure

measured at a height of 4 to 5 ft. In addition, flat surfaces of polyfoam must be kept to a minimum in the immediate vicinity of the model for reasons to be discussed shortly. The sectional column approach permits measurements at all frequencies to benefit from the relatively large investment that is required for a precision mount and its controls. If measurements are anticipated involving very heavy models as well as small ones, the additional cost of acquiring two mounts of different size and capability will usually be rapidly recovered in convenience that leads to reduced measurement times. The average reduction in time per measurement may be only 2 to 3 min, but it typically involves at least two people and is repeated many times each year so that the cost saving rapidly multiplies.

Sections of the polyfoam column can generally be fitted together by turning the cavity and extensions of adjoining sections in a lathe. The fit must be good and it is a high wear connection but changes are not made very frequently.

The overriding requirement of the entire model support structure is that it be free of random wobbles if the system is to be used for measurements of phase. At 10 GHz, for example, the wavelength is 1.18 in. and one degree of phase corresponds to 1.18/360 = 0.0033 in. While a random wobble of ±1/16 in. will have no measurable effect on power or amplitude measurements at 10 GHz, it would introduce an error of ±2 (0.0625/0.0033) = ±38° in measurements of phase. The factor of 2 is introduced because of the two way path. At 40 GHz, the phase error introduced by a 1/16 in. wobble is four times as great or ±152°.

5.1 The Mount

The principal requirements of the mount are (1) that it be capable of handling the heaviest models to be measured, (2) that it be capable of precision control of at least 0.1° in azimuth, (3) that it be fitted with wheels or castors for easy movements in at least two orthogonal directions, (4) that it be rock steady when locked in position, and (5) that it be compatible with control and data processing equipment that will be used. A number of commercially available antenna testing mounts fulfill these accuracy requirements and are available in a wide range of sizes. In addition they are designed to interface with a wide assortment of data handling equipment from traditional analog pattern recorders to sophisticated computers that provide both programmed control of the mount motion and programmed real time manipulation of the data. Generally, the more automated mounts are most cost effective when a large number of basically repetitive measurements are anticipated.

The precision rotation capability is required for measurements at high frequencies and measurements of phase. Consider, for example, the measurement of a 1 ft scatterer at 40 GHz. The scatterer will be essentially uniformily illuminated. If the scatterer is a circular metal disk the half power beamwidth of its principal backscatter lobe will be given approximately by 1/2 of the beamwidth of a circular antenna with uniform illumination, Eq. (14b). With $f = 40$ GHz, $\lambda =$ $\lambda = 0.295$ in., and $1/2\ \theta_{1/2} = 0.72$. This is the total angle between half power beamwidths of the principal backscattered lob. Clearly, a mount with azimuth control accuracy of 0.1° is barely adequate for such measurements. The phase tends to be relatively constant across principal lobes but to change rapidly near the edges of the beam. If the phase is to be sensibly tracked at all through these regions the mount accuracy must be at least 0.1°.

5.2 Basics of Polyfoam Columns

Columns of foamed polystyrene are the most widely used supports for scattering models of up to a few hundred pounds in weight. Foamed polystyrene has a very low relative dielectric constant ranging from about 1.02 to 1.10 therefore low backscattering, although as will be shown, the backscatter is by no means negligible.

If experiments are centered vertically in the chamber, the required column supports could easily be as much as 7 ft long to extend from the top of the mount to the vertical center of the chamber less half the model's vertical thickness so that the model is centered in the antenna beam. In addition, columns of several different thicknesses would be convenient to accommodate both large and small models. Unless a completely new column is to be used for each different model,

a section of about 1 ft in height should be replaceable because the top of the column will generally require special shaping to hold each different model.

Thin foamed polystyrene columns tend to bend even under their own weight if they are more than 18 to 24 in. in length. Therefore, the complete column might be fabricated in sections to permit a sturdy low cross section base and use of a thinner upper section for small models. Several designs are possible of which a typical one is shown in Figure 16. Ultimately, having several columns that can be interchanged on the mount base for different classes of measurements will prove to be very convenient.

The foamed material generally comes in blocks and the columns must be cut and turned from the blocks and planks. Procedures have included rough cutting with a saw and final turning on a lathe with sandpaper as the cutter, and cutting with a hot wire saw. The material generally dulls regular lathe cutting tools too rapidly to make their use practical. Also, the columns tend to bend away from the force of a cutting tool.

The columns must be absolutely circularly symmetric and mounted in the center of rotation of the mount. One method of achieving centering of a smaller column has been a series of guy strings attached to the column and a broad mount base at 120° angular intervals. The reason for the required centering care is that even through backscatter from the column is small, it eventually becomes the dominant term in the background signal as other sources of background scattering are canceled. Any forward or backward motion of the column as it revolves through a pattern can disturb seriously the cancellation level. A digital cancellation scheme that subtracts the background signal from the target signal might reduce these tolerances and would be feasible if the facility were equipped for storing the signal phase and amplitude on tape for later computer processing, or if the facility were equipped for real time data manipulation with sufficient storage.

In so far as practical it is recommended that experiments be centered vertically below the vertical center of the chamber if vertical centering requires a ladder or steps to reach to model. This might be practical at frequency bands from about 8 GHz to 12 GHz and higher. The lower centering of the experiment simplifies fabrication of the column and significantly reduces the physical effort of placing the model on the mount and removing it from the mount, if the experiment permits the model change without the use of steps. In the course of a good day of data taking the process of placing the model on the mount, removing it, placing a reference scatterer on the mount, may be repeated several hundred times and climbing even three or four steps to reach the top of the mount each time is very tiring by the end of the day.

5.2.1 COLUMN DIAMETER VS MODEL WEIGHT

A conservative relation that defines the diameter of a polyfoam column of height h to support a weight W is[7]

$$d = 8(h/\pi)^{1/2}(W/\pi E)^{1/4} \tag{54}$$

where E is the elastic modulus and a factor of 2 has been added for safety. A conservative value of the elastic modulus for styrofoam is 1500 psi.

As an example, W = 25 lb, h = 8 ft

$$d = 8(96/\pi)^{1/2}\left(\frac{25}{\pi\, 1500}\right)^{1/4} = 11.9 \text{ in.}$$

5.2.2 BACKSCATTER-CYLINDRICAL COLUMN

The following argument is very approximate but it is simple and works quite well. Polyfoam has very low losses. Therefore a plane wave incident on a column of polyfoam is reflected from both the front and back surfaces and the reflections are about equal in amplitude but the reflection from the back surface has a phase lag approximately equal to the total electrical path through the material. Assume the front and back surfaces to be planar. Then[8]

$$\sigma(o) = \frac{1}{2}\, kdh^2 \left|1 - j\, e^{j2kd\sqrt{\epsilon}}\right|^2 |R(o)|^2 \tag{55}$$

where d is the column diameter, h is the length, and R is the reflection coefficient for planar surfaces at normal incidence,

$$R = \frac{\sqrt{\epsilon} - \sqrt{\mu}}{\sqrt{\epsilon} + \sqrt{\mu}} \doteq 1/4(\epsilon - 1) \tag{56}$$

since $\mu \doteq 1$ and $(\epsilon - 1) \ll 1$.

$$\sigma(o) = \frac{kdh^2}{16}\, (\epsilon - 1)^2 \{1 + 2 \sin [2kd\sqrt{\epsilon}]\} \ . \tag{57}$$

---

7. Knott, E. F. and Senior, T. B. A. (1964) Studies of Scattering by Cellular Plastic Materials, Report No. 5849 -1 -F. The Radiation Laboratory, Univ. of Mich., Ann Arbor, Mich.

8. Senior, T. B. A., Plonus, M. A., and Knott, E. F. (1964) Designing foamed plastic target supports, Microwaves, 38-43.

Note that Eq. (57) has a maximum of

$$\sigma_{max} = \frac{kdh^2}{8}(\epsilon - 1)^2 \tag{58}$$

when

$$2kd\sqrt{\epsilon} = (4n + 1)\,\pi/2 \tag{59}$$

$$f_{max} = \frac{0.3(4n + 1)}{8d\sqrt{\epsilon}} \tag{60}$$

where f_{max} is the frequency in GHz corresponding to a maximum, and d is the column diameter in meters.

Equation (57) also has a minimum of zero when

$$2kd\sqrt{\epsilon} = (4n - 1)\,\pi/2 \tag{61}$$

or

$$f_{min} = \frac{0.3(4n - 1)}{8d\sqrt{\epsilon}} \quad . \tag{62}$$

Typical σ_{max} for columns are given in the following examples:

h = 8 ft, ϵ = 1.05, d = 14 in.

f_{max} = 10.39 GHz, σ_{max} = 0.14 m^2 = -8.42 dBSM

with the same column but lower dielectric = 1.02,

f_{max} = 10.55 GHz, σ_{max} = -11.8 dBSM

The most significant point from Eqs. (57), (60), and (62), is that the column can be tuned to yield a minimum backscatter cross section at an infinite set of frequencies, and at higher frequencies successive values of f_{min} are reasonably close together. Several of the adjacent minima of the preceding example, for example, are (from Eq. (62))

f_{min} = 8.73, 9.36, 9.57, 9.99, 10.41, 10.83 GHz .

Although Eq. (57) was derived for normal incidence, it holds approximately over a small angular interval near normal so that it generally applies to all of the column that is within the antenna beam.

The values of f_{min}, calculated or measured, are those values at which backscatter contributions from the column will be an insignificant part of the total background signal.

5.2.3 BACKSCATTER-TRUNCATED CONE COLUMN

For heavier models, the truncated cone is very useful form of column. It is also a useful column form for the bottom portion of a sectional column. The question becomes what cone angle to choose. A very approximate analysis yields simple and useful results. If the backscatter from the finite cylinder is considered not more than (for example) 30° from normal, the backscatter can be represented reasonably in product form. That is, the broadside backscatter of the column is multiplied by a pattern factor. Using the worst case of a broadside maximun, Eq. (58), and the standard column scattering factor

$$\sigma(\theta) = \frac{kdh^2}{8} (\epsilon - 1)^2 \left[\frac{\sin (kh \sin \theta)}{(kh \sin \theta)}\right]^2 . \tag{63}$$

This function has zeros, or minimum in practice, when

$$\theta = \sin^{-1} \left[\frac{N\pi}{kh}\right] , \quad N = 1, 2, \ldots . \tag{64}$$

Thus, in addition to tuning its thickness, backscatter from the column could be reduced by tilting the column. Tilting the column is not practical but the next best thing is to tilt the forward surface that is in immediate contact with the wave. Doing this over 360° leads to the truncated cone. Scattering from the side of the cone can be further reduced by serrating the sides of the cone.

5.2.4 FORWARD SCATTERING FROM POLYFOAM COLUMNS

Although polyfoam has very low relative dielectric constants at microwave frequencies and low backscatter, the specular forward scattering near grazing incidence is very large, a condition frequently overlooked in the use of polyfoam as supports both in antenna experiments and in scattering experiments. The result is that often more polyfoam is better than less.

Consider the Fresnel reflection formulas for a plane surface. Let θ_i be the angle of incidence measured from normal, and assume perfect dielectrics. Then, see Kerr, Chapt. 4[3]

$$E_{\perp}: \quad \Gamma_H = \frac{E_R}{E_i} = \frac{\cos\theta_i - \sqrt{\epsilon_2/\epsilon_1 - \sin^2\theta_i}}{\cos\theta_i + \sqrt{\epsilon_2/\epsilon_1 - \sin^2\theta_i}} \tag{65a}$$

$$E_{\parallel}: \quad \Gamma_V = \frac{E_R}{E_i} = \frac{\epsilon_2/\epsilon_1 \cos\theta_i - \sqrt{\epsilon_2/\epsilon_1 - \sin^2\theta_i}}{\epsilon_2/\epsilon_i \cos\theta_i + \sqrt{\epsilon_2/\epsilon_1 - \sin^2\theta_i}} \quad . \tag{65b}$$

Let medium 1 be air and medium 2 be polyfoam. Let $\theta_i \rightarrow 90^o$, grazing incidence. Then

$$\Gamma_H = \Gamma_V = -1 \quad . \tag{65c}$$

Note that Eq. (65c) is independent of E and, therefore, at these grazing angles, the polyfoam might just as well be a sheet of metal (in at least one polarization). Also note that Eq. (65c) extends over a small range of angles near 90^o.

From a practical view for scattering measurements, Eq. (65c) means two things. The first is more bad news about reflections from the back wall. The second is that a flat surface of polyfoam of even a few square inches should never be permitted near the scattering model if there is any possibility of forward scattering at grazing incidence falling on the model. Worst case examples include conespheres, ogives, prolate spheroids, or even spheres placed on flat column tops or slightly buried in flat sheets of polyfoam. The interfering results are easily measured at X-Band with spheres below ka's of about 1 to 2 where measured cross sections vary by 1 to 2 dB depending where the sphere is placed on columns having top diameters of 4 to 5 in.

The preceding discussion has been carried out in terms of polyfoam but all materials have a similar behavior. An absorber, for example, is commonly used to prevent reflections from the metal parts of the mount base as shown in Figure 16. The absorber is typically mounted on a thick plywood base that is fitted with legs to facilitate adjustments. In situations where the model is mounted only 4 to 5 ft above the floor or where the model has supporting structural pieces that must be shielded from the incident field, particular care must be exercised to insure that flat surfaces of the absorber pyramids do not forward scatter onto the model space. This is a siutation where even a crude probing of the field with the shield in place can pay high dividends by resolving mysteries of variations in the measured data.

Figure 17 shows the results of such a field probing when a shield of 18 in. pyramidal absorber was placed about 2 in. below the column top where a small

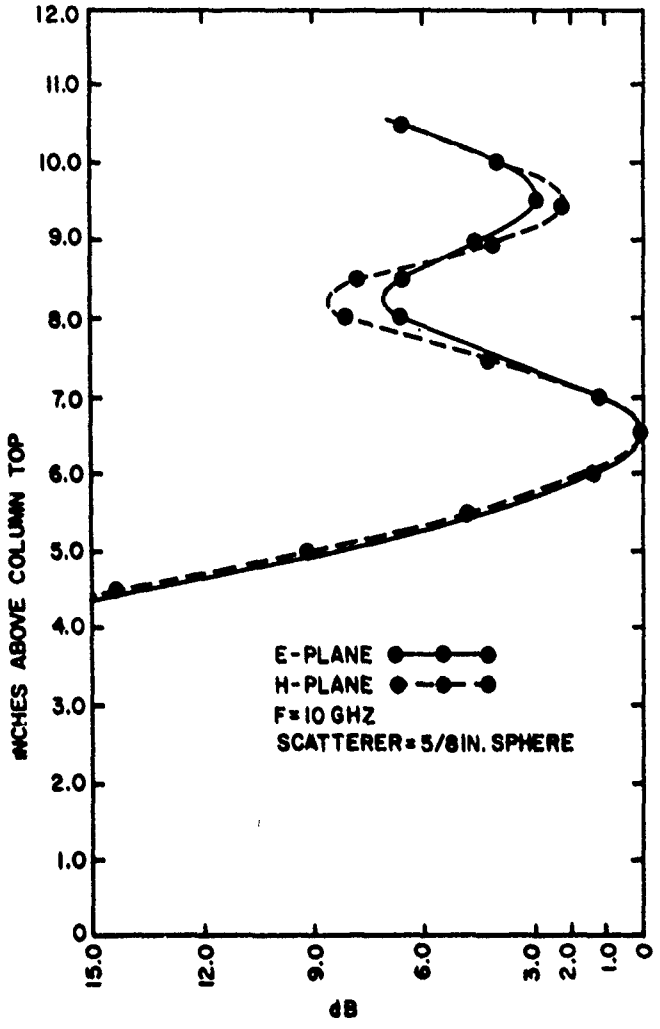

Figure 17. Variation of Power Over Model Space Due to Forward Scatter from Absorber Shield

model was to be located for measurement. The objective was to cover a small motor that was used to vibrate the model. The measurement frequency was 10 GHz and the scattering probe was a 5/8 in. diameter metal sphere. The sphere was suspended on a thin monofilament fishing line that in turn was hung over a polyfoam block setting atop the column. Half-inch spaces were marked in black crayon on the line and a corner of the polyfoam block was used as a position reference. Without the shield in place there was essentially no variation in the field over the region that was measured. As can be seen from Figure 17, the presence of the shield caused variations of as much as 8 dB even at distances of 8 in. or more above the shield.

6. RF POWER SOURCES

The principal requirements of an rf power source for a CW scattering measurement facility are that (1) it cover the correct frequency range, (2) it produce sufficient power, and (3) it have sufficient frequency stability and a sufficiently pure spectrum to permit useful cancellation levels to be maintained over the measurement times. In addition to the above, there are many applications for which an automated capability is advantageous and this imposes an additional requirement that the power source be compatible with the control equipment and other equipment with which it must interface.

The power requirements for a given set of measurements are easily determined from Eqs. (25), (28), or (32). The frequency stability requirements are not so easily stated, but the basis can be found from examining the CW cancellation process.

6.1 Cancellation Requirements

Let two signals that have traveled over different paths and through different components but that originate from the same source be brought together at the junction of a hydrid tee and their difference be observed in the difference arm of the tee. In general, each path has a different number of wavelengths and components whose rate of change of phase and attenuation with frequency differ for even small changes in frequency.

Let the two signals be represented as

$$e_A = A \cos (\omega t + \phi_A)$$

$$e_B = B \cos (\omega t + \phi_B) \tag{66}$$

where A and B designate, respectively, the two different paths. The net difference signal is

$$e = A \cos (\omega t + \phi_A) - B \cos (\omega t + \phi_B) \tag{67a}$$

$$= A [\cos (\omega t + \phi_A) - B/A \cos (\omega t + \phi_B)] \quad . \tag{67b}$$

Let the amplitude of the B-path signal be adjusted so that it differs from A by only a small amount Δ. Then

$$B = A + \Delta \quad , \quad \frac{B}{A} = 1 + \frac{\Delta}{A} \tag{68a}$$

and

$$\frac{e}{A} = \left[\cos(\omega t + \phi_A) - \cos(\omega t + \phi_B) - \frac{\Delta}{A}\cos(\omega t + \phi_B)\right] \quad (68b)$$

$$= -\left[2 \sin 1/2\,(2\omega t + \phi_A + \phi_B) \sin 1/2\,(\phi_A - \phi_B) + \frac{\Delta}{A}\cos(\omega t + \phi_B)\right] . \quad (68c)$$

For e to remain below some desired level over a measurement time, the difference $(\phi_A - \phi_B)$ and the ratio $\frac{\Delta}{A}$ must remain less than levels determined by Eq. (68c) for the measurement times. The maximum value of the coefficient of each is 1. Using this maximum or worstcase value and small angle approximations,

$$e_{dB} = 20 \log \left|\frac{e}{A}\right| = 20 \log \left|(\phi_A - \phi_B) + \frac{\Delta}{A}\right| \quad (69)$$

To illustrate the magnitudes involved in Eq. (69) consider the following examples. For simplicity, first consider $\Delta = 0$. Then if it is desired that e_{dB} remain below -100 dB over a measurement time, the phase difference $(\phi_A - \phi_B)$ must remain less than 0.00001 radian or 0.00058^o over this time period. Similarly for e_{dB} to remain less than -80 dB, $(\phi_A - \phi_B)$ must remain less than 0.0001 radian or 0.0058^o. (If $(\phi_A - \phi_B) = 0$, for a cancellation level of -100 dB Δ must be less than 10^{-5} and for a cancellation level of -80 dB Δ must remain less than 10^{-4}.

6.2 Frequency Stability Requirements

In a typical CW cancellation system the components of background signal cover the complete range between two extremes. On the one hand, there are directly coupled signals of relatively high amplitude but having a path length nearly equal to the path length of the signal used for cancellation. On the other hand, there are signals of much lower amplitude but that have traveled to the back wall and back and therefore have path lengths much greater than that of the canceling signal. For the latter components, long line effects increase frequency stability requirements as will be shown.

The fundamental concern with frequency stability is that it be sufficiently good that it is not the limiting factor in achieving and maintaining cancellation levels.

The following discussion is aimed at cancellation at rf. Let two signals be derived from the same transmitter at a directional coupler. A subscript A denotes the signal that has traveled through the transmission path and ϕ_A designates the total phase of this signal from the separation point. Similarly, a subscript B designates the reference cancellation signal that travels over a controlled path a through an attenuator and phase shifter that introduces an adjustable "trimming"

phase ϕ_C. The total phase of signal B except that introduced by the phase shifter is ϕ_B.

At the difference terminal of a hybrid the net signal is

$$\theta_A = A \cos(\omega t + \phi_A) \quad , \quad \theta_B = B \cos(\omega t + \phi_B + \phi_C) \tag{70a}$$

$$e = A \cos(\omega t + \phi_A) - B \cos(\omega t + \phi_B + \phi_C) \quad . \tag{70b}$$

Adjust the attenuator so that B = A. Then

$$e = A[\cos(\omega t + \phi_A) - \cos(\omega t + \phi_B + \phi_C)] \tag{70c}$$

$$= 2A \sin 1/2 (\omega t + \phi_A + \phi_B + \phi_C) \sin 1/2 (\phi_A - \phi_B - \phi_C) \quad . \tag{70d}$$

Clearly, e = o when

$$\phi_A - \phi_B - \phi_C = 2\eta\pi \tag{70e}$$

The phase terms are

$$\phi_A = \frac{2\pi\mathcal{L}_A}{\lambda} = \frac{2\pi\mathcal{L}_A}{c} f \tag{71a}$$

$$\phi_B = \frac{2\pi\mathcal{L}_B}{\lambda} = \frac{2\pi\mathcal{L}_B}{c} f \tag{71b}$$

where for simplicity an "adjusted" length $\mathcal{L}$ has been introduced to represent the free space path plus an adjusted path through transmission lines so that the free space propagation constant, $c = 3 \times 10^8$ m/sec can be applied to the entire path. The frequency is f.

Let the frequency be changed slightly from f to f + Δf. The new phases become

$$\phi'_A = \phi_A + \delta\phi_A = \frac{2\pi\mathcal{L}_A}{c}(f + \Delta f) = \frac{2\pi\mathcal{L}_A}{c} f + \frac{2\pi\mathcal{L}_A}{c} f \frac{\Delta f}{f} \tag{72a}$$

$$= \phi_A + \phi_A \frac{\Delta f}{f} \quad . \tag{72b}$$

Similarly,

$$\phi'_B = \phi_B + \delta\phi_B = \phi_B + \phi_B \frac{\Delta f}{f} \quad , \tag{72c}$$

$$\phi'_C = \phi_C + \delta\phi_C = \phi_C + \phi_C \frac{\Delta f}{f} \quad , \tag{72d}$$

$$\therefore \phi'_A - \phi'_B - \phi'_C = (\phi_A - \phi_B - \phi_C) + (\phi_A - \phi_B - \phi_C) \frac{\Delta f}{f} \quad .$$

With adjustments as originally set for complete cancellation, Eq. (70) gives

$$\phi'_A - \phi'_B - \phi'_C = 2n\pi + 2n\pi \frac{\Delta f}{f} \tag{73}$$

Note that in Eq. (73) the integer n functions as a counter that counts the number of phase cycles by which ϕ_A and ϕ_B differ since ϕ_C is a trimming phase that is adjusted to make the $(\phi_A - \phi_B)$ difference in integral multiple of 2π.

The question now is how much the Δf frequency upsets the cancellation level. From Eq. (70d),

$$\sin 1/2\,(\phi'_A - \phi'_B - \phi'_C) = \sin\left(n\pi + n\pi \frac{\Delta f}{f}\right) \tag{74a}$$

$$= \pm \sin\left(n\pi \frac{\Delta f}{f}\right) \tag{74b}$$

$$\doteq \pm (n\pi\, \Delta f/f) \text{ (for small angles)} \quad . \tag{74c}$$

At maximum uncanceled condition

$$e^2 = 4A^2 = P_c \tag{75}$$

where P_c is the power to be canceled. The second factor in Eq. (70d) is time dependent with a maximum of ±1. Therefore

$$|e|^2 = P_c \left|\sin 1/2\,(\phi'_A - \phi'_B - \phi'_C)\right|^2 \tag{76a}$$

$$= P_c \left|\sin (n\pi\, \Delta f/f)\right|^2 \quad . \tag{76b}$$

Let

$$\mathcal{E}_{dB} = 20 \log |e|$$

Then

$$\mathcal{E}_{dB} = P_{cdB} + 20 \log|\sin (n\pi\Delta f/f)| \tag{77a}$$

$$\doteq P_{cdB} + 20 \log (n\pi \Delta f/f) \quad . \tag{77b}$$

Consider three extreme examples:

1. Let paths A and B be essentially the same, R = 1, but the power to be canceled quite high, P_c = 5 mW, assumed to be half the transmitted power of 10 mW (10 dBm).

$$\therefore \quad R = 1 \quad , \quad P_c = 5 \times 10^{-3} \text{ w} = -23 \text{ dBw} = 7 \text{ dBm}$$

$$\mathcal{E}_{dB} \doteq 17 + 20 \log \Delta f/f$$

$\Delta f/f$	$\mathcal{E}_{dBm}$
10^{-5}	-83
10^{-6}	-103
10^{-7}	-123

In this case, a short term stability of 10^{-7} for $\Delta f/f$ would be at the limits of sensitivity of typical receivers. If the transmitter were 1 W this stability level would insure cancellation levels of -93 dBm instead of -123 dBm.

2. For this example let path A correspond to a signal that has traveled the length of the chamber and returned, $\mathcal{L}_A$ = 75 ft and $\mathcal{L}_B$ = 2 ft. Also let f = 10 GHz, and the power level $P_c = P_t$ - 30 dB. Assuming P_t = 10 dBm, P_c = -20 dBm.

$$\phi_A = \frac{2\pi\mathcal{L}_A}{\lambda} = \frac{2\pi(75)(12)}{1.18} = 4792.260$$

$$\phi_B = \frac{2\pi\mathcal{L}_B}{\lambda} = \frac{2\pi(24)}{1.18} = 127.794$$

$\phi_C = 0.373(2\pi) = 2.343$ rads.

n = 742

$\mathcal{E}_{dB} = -20 + 20 \log (742\pi \Delta f/f)$

$\Delta f/f$	$\mathcal{E}_{dB}$
10^{-5}	-52.65
10^{-6}	-72.65
10^{-7}	-92.65
10^{-8}	-112.65
10^{-9}	-132.65

Thus, even though the power to be canceled is much lower, the long line effects impose more stringent stability conditions.

3. The frequency is 1 GHz, with other conditions as in (2).

$\phi_A = 2\pi(75) = 471.239$

$\phi_B = 2\pi(2) = 12.566$

$\frac{\phi_A - \phi_B}{2\pi} = 458.673$

$\therefore \phi_C = 0.673(2\pi) = 4.266$ rads.

$\mathcal{E}_{dB} = 23.2 + 20 \log \Delta f/f$

$\Delta f/f$	$\mathcal{E}_{dB}$
10^{-5}	-76.8
10^{-6}	-96.8
10^{-7}	-116.8
10^{-8}	-136.8

Thus, the wavelength that is larger by roughly an order of magnitude, relaxes stability requirements by roughly an order of magnitude.

7. TRANSMISSION LINE COMPONENTS

Even with most expensive rf power sources, receivers, and mount equipment the complete key to accurate, repeatable, and efficient radar scattering measurements is in proper assembly of high quality transmission line components. Here efficiency is important. A good assembly of transmission line components permits rapid and sure adjustment of the cancellation level whereas a poor assembly makes achievement of the cancellation levels slow and tedious. This is a process that will be carried out tens of thousands of times over the life cycle of an equipment assembly, and the difference between 1 to 2 min vs 10 to 15 min is very significant in terms of long term operation costs. In addition, inability to easily achieve good cancellation tends to lead to relaxed standards overall for measurement results.

The above holds true even if digital cancellation techniques are used and because these techniques assume absolutely no change in phase or amplitude through the transmission line paths during the measurement times. In addition, most receivers have saturation levels that are below the initial uncanceled levels of the signals to be canceled. Hence, initial cancellation will probably be necessary either at the if or rf levels and this adjustment must remain constant during the measurement time.

Block diagrams showing the components required for both single transmit/receive antenna and dual transmit/receive antenna operation are given in Figures 18 and 19. These are more or less standard setups for such operation and variations are possible.

The components should be high quality and free of transmission changes due to vibration and small shock. The assembly for each frequency band should be firmly mounted on a base. Although the base can be metal, a thick plywood base is preferable because it reduces conduction paths. The plywood should be at least 3/4 in. thick and preferable 1 in. thick (formed by gluing together 2-1/2 in. thicknesses).

All joints between individual waveguide or coaxial components should be sealed; waveguide joints should be always choke to flange. However, even these leak some rf and should be further sealed. One technique that provides an effective sealing procedure for waveguide junctions consists of coating both flange and choke with thin coats of silver conducting paint, waiting until the paint is tacky, and then bolting the junction together.[9] The silver conducting paint used was Dupont Silver Preparation Electronic Grade 4922. Upon disassembly and reassembly, junctions so treated must be completely cleaned of the paint and the paint reapplied to insure

---

9. Mack, R.B., Wojcicki, A.W., and Andriotakis, J.J. (1973) An Implementation of Conventional Methods of Measuring the Amplitude and Phase of Backscattered Fields, AFCRL-TR-73-0418, AD 770 015.

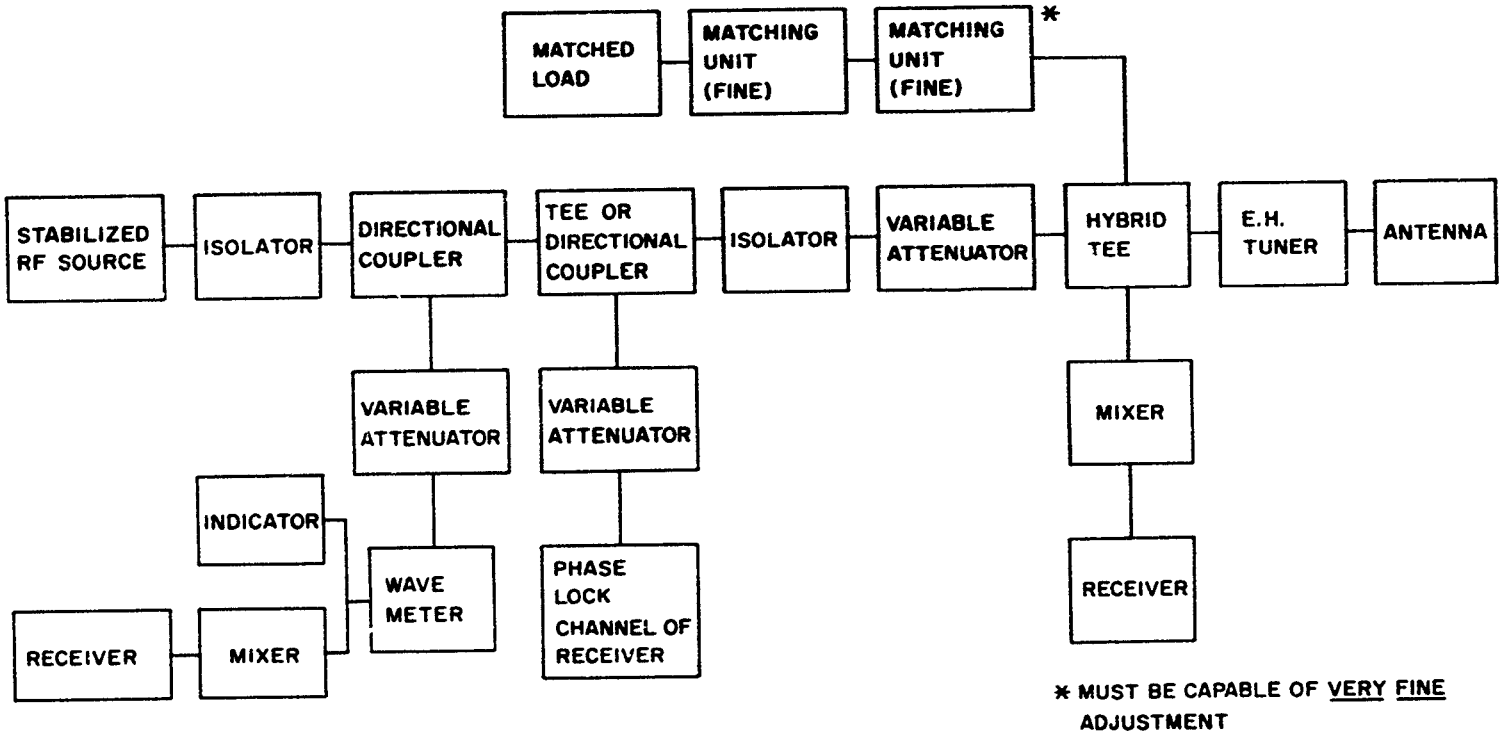

a. Matching Unit Cancellation

Figure 18. Single Antenna Backscatter Equipment

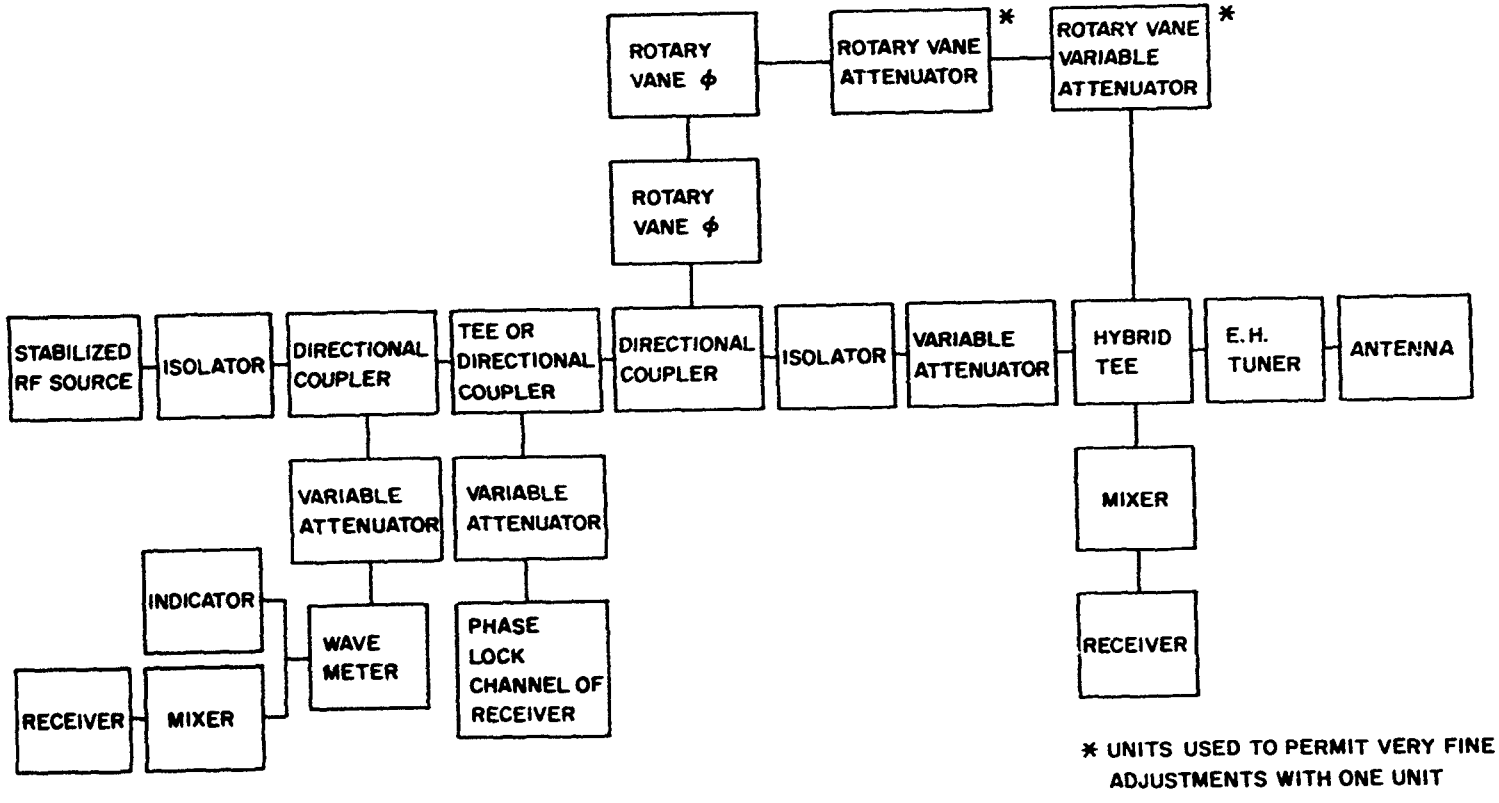

b. Phase Shifter/Attenuator Cancellation

Figure 18. Single Antenna Backscatter Equipment

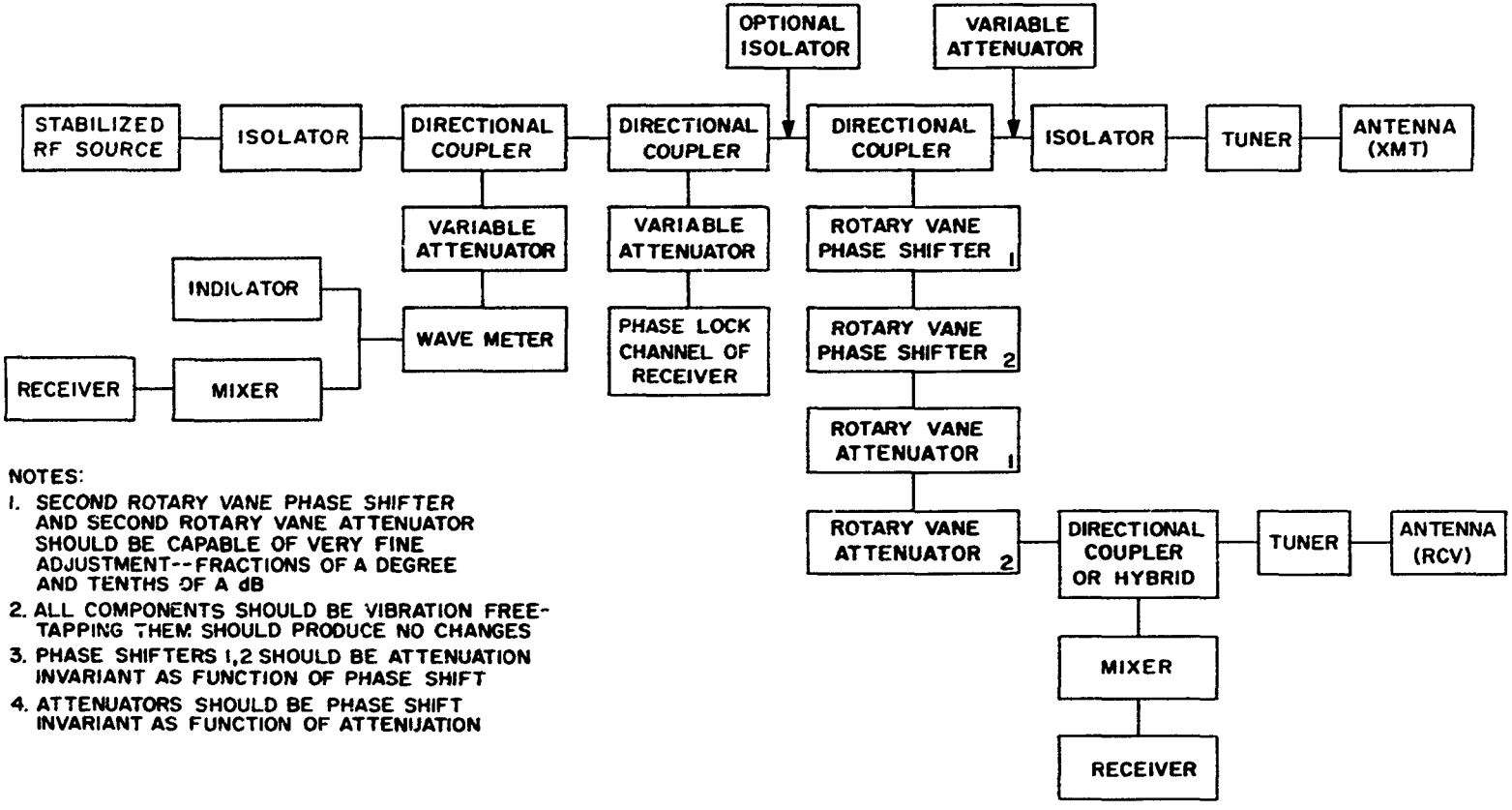

Figure 19. Dual Transmit/Receive Antenna Scattering Equipment Assembly

a good seal. For this reason the assembly should be first put together with regular bolted joints until final arrangement of the pieces is settled.

Avoid flexible coaxial line and, insofar as possible, flexible waveguide. At 2 GHz and above all rf lines from the transmitter output should be rigid coaxial line or waveguide with connecting pieces fabricated to fit. Even short sections should be adequately supported so that they are vibration free. Flexible coaxial lines from the mixers to receivers have not been found to cause any problems as long as they are within loss tolerances specified by the receiver manufacturer.

It is assumed that the assembly for each frequency band will be permanently assembled on its own base and for use slide into equipment racks located in the rf equipment space (Figure 4). These racks must be very solid with no motion or vibration and rock steady. For the lowest frequencies at least, the experiments will be centered vertically in the chamber, so the racks must be perhaps 10 ft tall. Because of the desirability of operating at lower heights whenever possible, it is recommended that the racks be of modular construction with top sections removable. The equipment assemblies on their base could slide into grooves in the racks, held in place securely by spring tensional rubber rollers. A personnel stand and stairs with railings to permit comfortable working height and meeting safety requirements will also be required. It is recommended that this stand be completely separate from the equipment rack so that motion by personnel on the stand cannot cause even the slightest movement of the equipment rack.

The transmitting source should be located close to the transmission line assembly and could well be located in the lower portion of the equipment rack, thereby helping to provide stability for the rack.

As mentioned earlier, if slide-in capability for several transmission line assemblies is provided in the rack, it might be possible to leave several assemblies including their antennas permanently in place. In some cases, at least, antennas will be mounted separately from the equipment and the possibility of small vertical movements of the equipment assemblies should be provided for purposes of alignment. For assemblies not in current use, slide-in storage racks should be provided in the rf equipment space. A sketch of one possible general form of the equipment rack is given in Figure 20.

In addition to the components shown in Figures 18 and 19, a bench test setup will be needed for each frequency band. At a minimum this should consist of a slotted line, probe, SWR meter, waveguide to coaxial adaptors, and at least one extra matched load. A power meter with thermistor or other appropriate heads for each band should be available.

Also, in addition to the components identified in Figures 18 and 19, a number of E and H plane 90° bends will be necessary along with several feet of waveguide and separate flanges and chokes so that sections of connecting waveguide can be

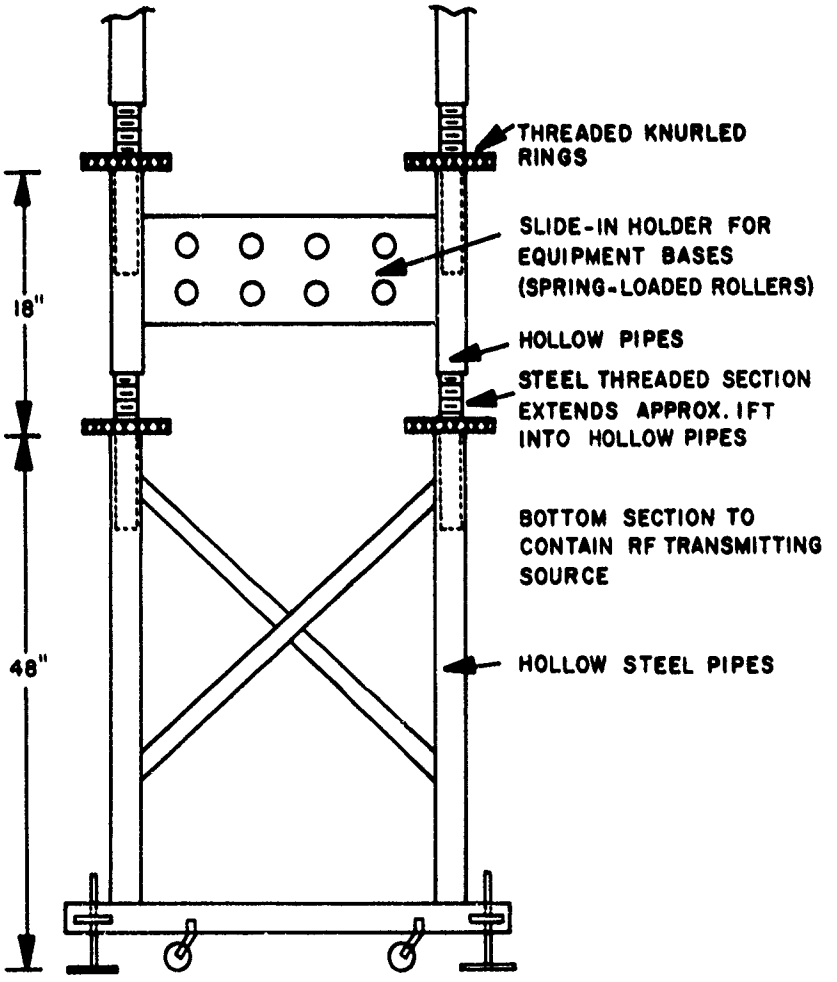

Figure 20. Equipment Racks

fabricated as necessary to connect the components, and to connect the rf source to the assembly.

A coaxial assembly will be the most convenient for frequencies from 1 GHz to 4 GHz and may be usable to 8 GHz. However, use beyond 4 GHz is unlikely. Therefore, waveguide assemblies will probably be needed for 4 to 8 GHz and 8 to 12 GHz but use of coaxial components to 8 GHz is worth trying, provided sufficient bandwidth can be found in all of the necessary components.

The following list includes sufficient components for any of the assemblies of Figures 18 or 19. The components are listed in terms of waveguide but in most cases direct coaxial line equivalents can be found. In the case of tees and bends, fewer coaxial ones would be needed because there is no E or H plane distinction.

Table 7. List of Transmission Line Components

Quantity	Item	
3	Isolators	
4	Directional couplers (1 to 10 dB, 1 to 20 dB, 2 to 40 dB)	
2	Variable attenuators (0 to 50 dB or 0 to 100 dB, uncalibrated)	
1	Variable attenuator, calibrated (0 to 50 dB)	
2	Rotary Vane Precision Attenuator (1 - 0 to 100 dB, 1 - 0 to 10 dB preferred)	
2	Rotary vane precision phase shifters	
2	E. H. tuners	
1	180° hybrid (very high quality, solid)	
2	Matching units, very fine adjustments (3 or 4 preferable for higher frequencies)	
4	Matched loads (3 needed, 1 optional)	
5	E-Plane 90° bends	Some number of these will be required for assembly. If a laboratory stock is available, these components can be drawn from that stock.
5	H-Plane 90° bends	
3	E-Plane tees	
3	H-Plane tees	
1	3 ft section waveguide	
12	ea flanges and chokes	
Optional but Needed for Occasional Use		
1	Slotted line with probe (or network analyzer)	
2	Waveguide to coaxial adaptors	
1	Matched load	
1	SWR meter	
1	Power meter	

8. TYPICAL FACILITY PERFORMANCE

The purpose of this section is to show examples of the minimum cross sections having errors of no more than ±1 dB that can be measured on a typical backscatter facility. The parameters chosen for the facility do not apply to any specific equipment but are typical of the state of the art commercially available components. The parameters of the measurement system and the resulting minimum measurable cross sections in square meters are summarized in Table 8 for both optimum antennas and for the three-antenna approximation that was discussed in Section 6.

Table 8. Assumed Typical Equipment Parameters and Minimum Measurable Cross Sections

Freq. (GHz)	Equipment Parameters				σ_{min} (m^2)	
	Receiver Sensitivity (dBm)	RF Power Source Output (dBm)	Antenna Gain (dB)		Opt Ant (±1 dB Error)	3 Dish Appr. (±1 dB) Error)
			Optimum	3 Dish Appr.		
1.0	-105	+10	19.8	17.4	-39.6	-34.8
2.0	-105	+10	22.8	23.4	-39.6	-40.8
4.0	-100	+10	25.8	29.4 (23.4)	-34.6	-41.7 (-29.7)
8.0	-95	+10	28.9	29.5	-29.7	-30.9
12.0	-90	+10	30.6	33.0 (29.5)	-24.5	-29.4 (-22.4)
15.0	-90	+10	31.6	31.4	-24.7	-24.3
18.0	-90	+10	32.4	33.0	-24.7	-25.9
22.0	-85	+10	33.3	34.7	-20.0	-22.5
26.0	-85	+8	34.0	36.2	-17.7	-22.1
33.0	-80	+8	35.0	38.2	-12.6	-19.0
40.0	-70	+6	35.6	39.9	-0.1	-18.7

α = 12 dB; R = 32 ft = 9.754 m

Assumptions underlying the calculations are:

1. The measurement system is a backscatter facility with a single transmit/receive antenna.

2. The maximum useful range for measurements is R = 32 ft (9.754 m) and all measurements are made at this range.

3. The antennas are 60 percent efficient with gains given by Eqs. (50) and (53).

4. There is a total loss of 12 dB in the transmission line components. This is composed of a 6 dB loss in the hybrid tee, a 5 dB loss in the detecting or mixing crystal, and 1 dB of miscellaneous losses.

5. The minimum detectable signal of the receiver and the output of the signal generator vary over the frequency band of 1 GHz to 40 GHz approximately as shown in Table 8.

6. Miscellaneous background reflections and the uniformity of the incident field over the model space are not the factors limiting measurement accuracy.

7. The minimum measurable reflected signal must be 20 dB greater than the minimum detectable signal of the receiver, resulting in a ±1 dB uncertainty in the measured results.

The resulting minimum measurable cross sections, σ_{min}, in square meters are shown in Figure 21 as a function of frequency for both optimum antennas and for the three-antenna approximation. As can be seen from Table 8, the decrease in minimum measurable cross sections at the higher frequencies is due to the assumed decrease in the receiver sensitivity and output of the signal source at the higher frequencies. The use of stable amplifiers to boost the output of the signal source would improve σ_{min} at these frequencies in a direct relation to the gain of the amplifier.

The scale factor from 1 GHz to 40 GHz is 40, or 1600 in area, and equivalent to 32 dB. Hence, with the 12 in. dish, cross sections of about 13.3 dBSM or 2.14 m^2 at L-Band could be scaled to 40 GHz and measured with a ±1 dB error. Similarly, with the 18 in. dish, L-Band cross sections of about 0.1 m^2 could be measured at 10 GHz, while L-Band cross sections as low as -35 dBSM could be measured at L-Band directly.

In Figure 22 the maximum antenna size, the maximum model size, and the working distance between half power points of the beam at the model space are shown as a function of frequency for measurement ranges from R = 32 ft to R = 72 ft. These curves are based on the conventional far field criterion. If half of this distance is to be used for measurements, $R = D^2/\lambda$ instead of $R = 2D^2/\lambda$, the resulting antenna size is multiplied by a factor of approximately 1.4. This value can be obtained from Figure 22 by choosing the antenna size corresponding to a value of R that is twice as large at the desired frequency.

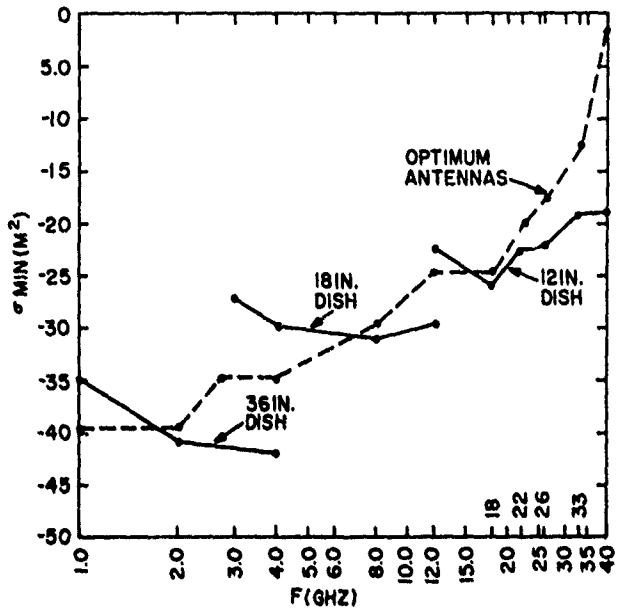

Figure 21. Minimum Measurable Cross Sections with ±1 dB Error with Typical Backscatter Facility (for facility parameters see Section 8)

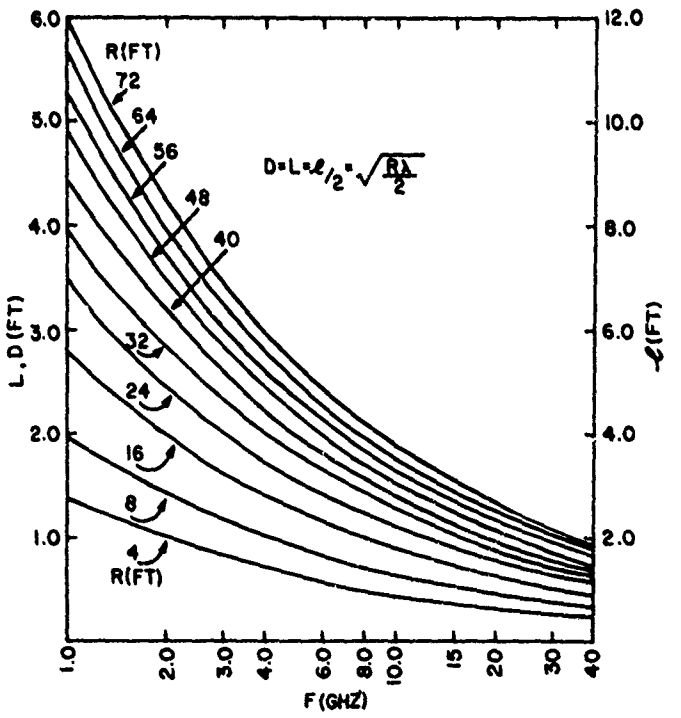

Figure 22. Maximum Model Size, Maximum Antenna Size, and Half Power Beam Distances for f = 1 GHz to 40 GHz at Various Measurement Distances

References

1. Blacksmith, P., Hiatt, R.E., and Mack, R.B. (1965) Introduction to radar cross section measurements, Proc. IEEE 53:901-920.
2. Silver, S. (1949) Microwave Antenna Theory and Design, Vol. 12, Radiation Laboratory Series, McGraw-Hill Book Company, Chap. 6.
3. Kerr, D.E. (1951) Propagation of Short Radio Waves, Vol. 13, Radiation Laboratory Series, McGraw-Hill Book Company, Chapts. 4 and 6.
4. Skolnik, M.I. (1968) Introduction to Radar Systems, McGraw-Hill Book Company, Chapts. 1 and 7.
5. Van De Hulst, H.C. (1957) Light Scattering by Small Particles, John Wiley & Sons, Inc., New York, Chapt. 9.
6. Freeny, C.C. (1966) Target support parameters associated with radar reflectivity measurements, Proc. IEEE 53:929-936.
7. Knott, E.F. and Senior, T.B.A. (1964) Studies of Scattering by Cellular Plastic Materials, Report No. 5849 -1 -F. The Radiation Laboratory, Univ. of Mich., Ann Arbor, Mich.
8. Senior, T.B.A., Plonus, M.A., and Knott, E.F. (1964) Designing foamed plastic target supports, Microwaves, 38-43.
9. Mack, R.B., Wojcicki, A.W., and Andriotakis, J.J. (1973) An Implementation of Conventional Methods of Measuring the Amplitude and Phase of Backscattered Fields, AFCRL-TR-73-0418, AD 770 015.